İSTANBUL TECHNICAL UNIVERSITY ★ INSTITUTE OF SCIENCE AND TECHNOLOGY

ANALYSIS AND DESIGN OF A LONG SPAN CABLE-STAYED BRIDGE

M.Sc. Thesis by
Müge KULELI

Department : Civil Engineering

Programme : Structural Engineering

Thesis Supervisor: Assis. Prof. Dr. B. Ozden CAGLAYAN

JUNE 2011

İSTANBUL TECHNICAL UNIVERSITY ★ INSTITUTE OF SCIENCE AND TECHNOLOGY

ANALYSIS AND DESIGN OF A LONG SPAN CABLE-STAYED BRIDGE

M.Sc. Thesis by
Müge KULELİ
(501081091)

Date of submission :	**06 May 2011**
Date of defence examination:	**10 June 2011**

Supervisor (Chairman) :	**Assis.Prof.Dr.B. Ozden CAGLAYAN(ITU)**
Members of the Examining Committee :	**Prof. Dr. Zekai CELEP (ITU)**
	Prof. Dr. Faruk YÜKSELER (YTU)

JUNE 2011

İSTANBUL TEKNİK ÜNİVERSİTESİ ★ FEN BİLİMLERİ ENSTİTÜSÜ

KABLO ASKILI KÖPRÜLERİN ANALİZ VE TASARIMI

YÜKSEK LİSANS TEZİ
Müge KULELİ
(501081091)

Tezin Enstitüye Verildiği Tarih : 06 Mayıs 2011
Tezin Savunulduğu Tarih : 10 Haziran 2011

Tez Danışmanı : Yrd.Doç.Dr.B. Ozden ÇAĞLAYAN(İTÜ)
Diğer Jüri Üyeleri : Prof. Dr. Zekai CELEP (İTÜ)
Prof. Dr. Faruk YÜKSELER (YTÜ)

HAZİRAN 2011

FOREWORD

I would like to express my special thanks to my advisor, Assist. Prof. Dr. Barlas Ozden Caglayan, for his guidance and encouragement throughout this work. This thesis would not be possible without his support for my academic goals.

I would also acknowledge the generous discussions and support provided by my experienced collegeue and friend, Mr. Ovunc Tezer.

I would also express my deepest gratitude to my dearest friend Mr. Berkin Ozgeneci for his enduring support, encouragement and patience during my academic studies.

Finally, I wish to dedicate this thesis to my mother, Belgin, my father, Teoman, and my brother, Mete, who have always stood by my side and given their unconditional love. I would not be able to achieve any of my goals without their encouragement and endless belief in me.

May 2011 Müge KULELİ

(Civil Engineer)

TABLE OF CONTENTS

Page

TABLE OF CONTENTS .... **vii**
ABBREVIATIONS .... **ix**
LIST OF TABLES .... **xi**
LIST OF FIGURES .... **xiii**
SUMMARY .... **xv**
ÖZET .... **xvii**
1. INTRODUCTION **1**
1.1 The Origin of the Thesis 1
1.1 Incheon Bridge, Korea 1
1.1 Tatara Bridge, Japan 3
2. CABLE-STAYED BRIDGE CONFIGURATION **5**
2.1 Configuration of Cable-Stayed Bridges 5
    2.1.1 General Layout 5
    2.1.2 Towers and Spatial Cable Layout 6
    2.1.3 Stiffening Girder 8
    2.1.4 Cables and Anchorages 10
    2.1.5 Foundations 12
3. STATE OF RESEARCH ON CABLE-STAYED BRIDGES **13**
  3.1 Nonlinearities in Cable-Stayed Bridges 13
  3.2 Dynamic Characteristic and Response 15
  3.3 Damping Characteristics 18
4. BRIDGE CONFIGURATION **23**
  4.1 Structure Description 23
    4.1.1 The Deck 24
    4.1.2 The Pylons and Piers 26
    4.1.3 The Stay Cables 26
5. FINITE ELEMENT OF THE BRIDGE **27**
  5.1 Introduction 27
  5.2 Description of The Finite Element Model 27
    5.2.1 The Deck 27
    5.2.2 The Cables 31
    5.2.3 The Pylons and Piers 32
    5.2.4 The Foundations 32
  5.3 Static Loading Conditions 33
    5.3.1 Optimization of Cable Pretension 33
    5.3.2 Vehicular Live Load 37
  5.4 Earthquake Records 38
  5.5 Damping Characteristic 45
6. CHARACTERISTICS OF THE BRIDGE **47**
  6.1 Static Characteristics of the Bridge 47
  6.2 Dynamic Characteristics of the Bridge 47

7. EARTHQUAKE RESPONSE 51
7.1 Introduction 51
7.2 Nonlinear Time History Analysis 51
7.3 Results 51
8. CONCLUSIONS 61
REFERENCES 63
CURRICULUM VITAE 71

ABBREVIATIONS

AASHTO **:** American Association of State Highway and Transportation Officials
AISC **:** American Institute of Steel Construction

LIST OF TABLES

Page

Table 3.1 : Natural Frequcies of Meiko-nishi Bridge 16
Table 4.1 : Material properties 24
Table 4.2 : Rib cross-section properties 25
Table 5.1 : Stiffness properties of the box girder 28
Table 5.2 : Weight properties of the deck 29
Table 5.3 : Distances between distributed lumped masses and shear centre 30
Table 5.4 : Mass properties of the deck 31
Table 5.5 : The calculated equivalent modulus of elasticity of the cables 32
Table 5.6 : Loading Conditions 33
Table 5.7 : Load Combinations and load factors 33
Table 5.8 : Load factors for permanent loads, γ_p 33
Table 5.9 : Multiple Presence Factors *m* 37
Table 5.10 : PGA/PGV Ratio Range 40
Table 5.11 : Selected Ground Motions 41
Table 5.12 : Fundamental Periods of IY 700 41
Table 6.1 : Boundary Conditions 47
Table 6.2 : First 15 modes 48
Table 7.1 : Comparison of moment values for element 134 between code specified load combinations 59
Table 7.2 : Comparison of moment values for element 112 between code specified load combinations 59
Table 7.3 : Increment ratio for rotational displacement of node 70 59

LIST OF FIGURES

Page

Figure 1.1 : The Expressway Link (Korea)... 2
Figure 1.2 : Incheon Bridge Elevation... 2
Figure 1.3 : Incheon Bridge (Korea).. 2
Figure 1.4 : Tatara Bridge (Japan) 3
Figure 1.5 : Tatara Bridge Elevation.. 3
Figure 2.1 : Concept of a cable-stayed bridge 5
Figure 2.2 : Radial, harp and semi-fan (modified fan) arrangements for cable stayed bridge systems 6
Figure 2.3 : a) Two vertical plane b) Two inclined planes c) Single plane systems. 7
Figure 2.4 : A, H and Diamond configurations of Towers 8
Figure 2.5 : Cable span length – force relation.. 9
Figure 2.6 : Parallel wire cable 10
Figure 2.7 : Strand Cable. 10
Figure 2.8 : Locked-coil cable 11
Figure 2.9 : Anchorage of mono-strand cables to a concrete pylon 12
Figure 2.10 : Overlapping of stay cable anchorages... 12
Figure 3.1 : Nonlinear stress-strain relationship for a cable-stay 14
Figure 3.2 : Geometric hardeneing type.. 14
Figure 3.3 : Correspondence between modes from ambient vibration tests and from FE model 1C (linear analysis) and 17C (Geometric Nonlinear Analysis) 17
Figure 3.4 : Response comparison between linear and nonlinear analysis............ 18
Figure 3.5 : Meiko-nishi Bridge experiment model.. 20
Figure 3.6 : Comparison of damping ratio versus oscillation amplitude relation for longitudinal oscillation 21
Figure 3.7 : Comparison of damping ratio versus oscillation amplitude relation for vertical oscillation.. 21
Figure 4.1 : Elevation of IY 700 Bridge 23
Figure 4.2 : Cross-section of orthotropic steel box girder 24
Figure 4.3 : Cross-section of ribs.. 25
Figure 5.1 : Finite element model of the bridge.. 27
Figure 5.2 : Finite element model of the deck cross-section 28
Figure 5.3 : Finite element model of the deck 28
Figure 5.4 : Distribution of lumped masses used in calculating the total lumped masses 29
Figure 5.5 : Force – displacement relationship of cables...................................... 31
Figure 5.6 : Finite element model of a pylon.. 32
Figure 5.7 : Bending moment distribution in deck (dead load) 36
Figure 5.8 : Dead load deformed shape (scaled)... 36
Figure 5.9 : Cable Groups.. 36

Figure 5.10 : AASHTO-LRFD design truck 37
Figure 5.11 : Maximum and minimum bending moments in deck 38
Figure 5.12 : (a) Distribution of V/H Ratio; (b) time interval 41
Figure 5.13 : Time – acceleration of Imperial Valley vertical component 42
Figure 5.14 : El Centro Array #6 – Vertical Component Response Spectrum 42
Figure 5.15 : El Centro Array #6 – Vertical Component FFT 42
Figure 5.16 : Time – acceleration of Chi Chi vertical component 43
Figure 5.17 : Chi Chi Taiwan, TCU068 – Vertical Component Response Spectrum 43
Figure 5.18 : Chi Chi Taiwan, TCU068 – Vertical Component FFT 43
Figure 5.19 : Time – acceleration of Kocaeli vertical component 44
Figure 5.20 : Kocaeli, Yarimca – Vertical Component Response Spectrum 44
Figure 5.21 : Kocaeli, Yarimca – Vertical Component FFT 44
Figure 6.1 : Fundamental Mode, TL 1 47
Figure 6.2 : 2nd Mode, V 1 48
Figure 6.3 : 4th Mode, TL 2 48
Figure 6.4 : Period distribution 49
Figure 6.5 : Modal mass participation in longitudinal direction 49
Figure 7.1 : Element and node of girder considered at midspan for response 52
Figure 7.2 : Element and node considered at pylon section of girder for response 52
Figure 7.3 : E134 – My Moment 52
Figure 7.4 : N94 – Ry Displacement 53
Figure 7.5 : E112 – My Moment 53
Figure 7.6 : N70 – Ry Displacement 54
Figure 7.7 : E134 – My Moment 54
Figure 7.8 : N94 – Ry Displacement 55
Figure 7.9 : E112 – My Moment 56
Figure 7.10 : N70 – Ry Displacement 56
Figure 7.11 : E134 – My Moment 57
Figure 7.12 : N94 – Ry Displacement 57
Figure 7.13 : E112 – My Moment 58
Figure 7.14 : N70 – Ry Displacement 58

ANALYSIS AND DESIGN OF A LONG SPAN CABLE-STAYED BRIDGE

SUMMARY

In this study, the behaviour of long span cable-stayed bridges under the effect of static and dynamic loads is investigated.

First, a cable-stayed bridge configuration with 105+245+700+245+105 m span lengths is decided to represent today's trend which based on the knowledge and experience of the latest long span cable-stayed bridge projects. Preliminary design is carried out, and then the bridge is analysed under its own weight with the effects of the nonlinearities which cable-stayed bridges have inherently. Pretension optimization of cables is carried out and then the bridge is analysed under the effect of the vehicular live loads.

Near-fault ground motion datas are selected considering the appropriate criterias and nonlinear time history analysis is carried out to obtain the response of the bridge under the effects of only horizontal components of these selected ground motions.

Analyses with the contibution of the vertical components of the ground motions are also carried out. Change of internal forces and the rotational displacements are compared.

KABLO ASKILI KÖPRÜLERİN ANALİZ VE TASARIMI

ÖZET

Bu çalışmada, uzun açıklıklı kablo askılı köprülerin statik ve dinamik yükler etkisi altında davranışı incelenmiştir.

Öncelikle, son yıllarda inşaa edilmiş uzun açıklıklı kablo askılı köprü projeleri ve deneyimleri esas alınarak günümüz trendlerini temsil eden 105+245+750+245+105 açıklıklarına sahip bir köprü konfigürasyonuna karar verilmiştir. Köprünün ön tasarımı yapılmış kendi ağırlığı etkisinde lineer olmayan analizi yapılmıştır. Kablo ön çekme kuvvetlerinin optimizasyonu yapılmış ve hareketli araç yükleri etkisinde analizi yapılarak statik yükler etkisindeki tasarımı tamamlanmıştır.

Statik yüler etkisi altında tasarımı yapılan köprünün, lineer olmayan zaman tanım alanı yöntemi ile çeşitli deprem kayıtları kullanılarak yer hareketinin sadece yatay iki bileşeni etkisi altında analizi yapılmıştır. Yatay bileşenlere düşey bileşen de katılarak analiz tekrarlanmıştır. Yukarıda belirtilmiş olan iki dinamik etki altındaki iç kuvvet ve dönme yerdeğiştirme değerlerindeki değişim karşılaştırılmıştır.

1. INTRODUCTION

1.1 The Origin of the Thesis

Cable-stayed bridges has been a research subject for about two decades. One of the earlier research projects was conducted by Nazmy and Abdel-Ghaffar [1]. This report comprised two different span lengths with same bridge configuration which the shorter span was representing the 1980's trend and longer span was representing the future trend in design of cable-stayed bridges.

Multi-support excitation and the uniform excitation were considered. Nonlinearities due to different types of sources are included in analysis. In addition, a comparison between linear and nonlinear earthquake response analysis were carried out.

In this study, the configuration of the bridge is selected based on the latest long span cable stayed bridge projects, Incheon Bridge (Korea) and Tatara Bridge (Japan) to represent the current trend of long span cable stayed bridge projects.

The behavior of the bridges compared under the effects of only horizontal component near field ground motions and with the contribution of the vertical component to only horizontal case.

Especially the flexural moment and rotational displacement variations due to contribution of the vertical component of near fault strong ground motions are studied.

1.2 Incheon Bridge, Korea

Incheon Bridge is a long span cable stayed bridge with 80 + 260 + 800 + 260 + 80 m. span lenghts which is a part of Korean Expressway Link as shown in Figure 1.1.

A streamlined orthotropic box girder was adopted. Y shape concrete pylons with semi-fan type cable arrangement was employed. Cable stays were installed in two-sided with the spacing of 15m. The supplementary piers are separate hollow section twin columns and 58m in height. Counterweights are installed to resist the uplift forces at the end piers. [2], [3]. The elevation of the bridge is shown in Figure 1.2.

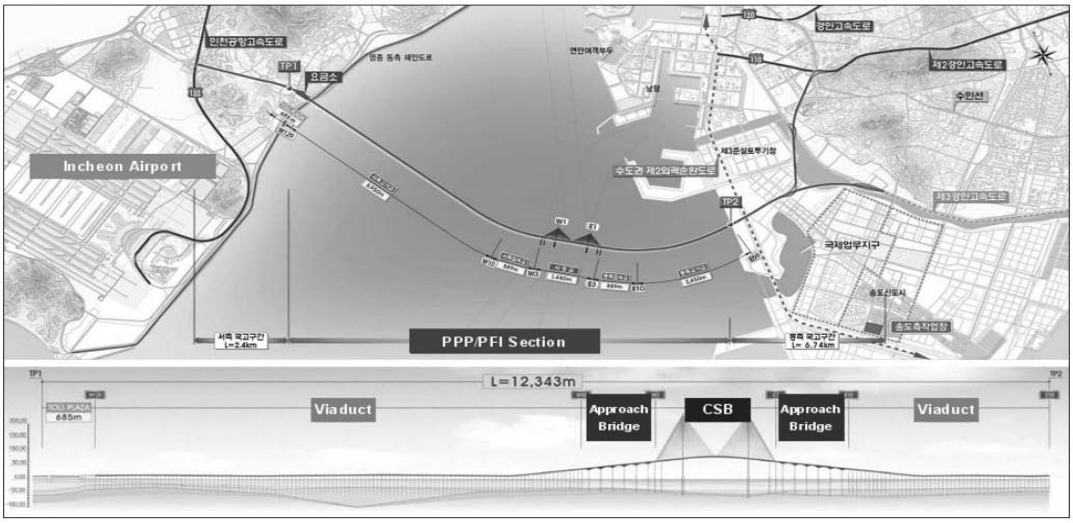
인천공항고속도로
TP1
요금소
영종 동측 해안도로
연안여객부두
남항
경인고속도로
제2경인고속도로
수인선
Incheon Airport
제3준설토투기장
수도권 제2외곽순환도로
TP2
제3경인고속도로
W1
E1
W10
W3
E3
E10
국제업무지구
송도신도시
송도측작업장
서측 국고구간
L=2.4km
PPP/PFI Section
동측 국고구간
L= 6.74km
TP1
TP2
L=12,343m
685m
Viaduct
Approach Bridge
CSB
Approach Bridge
Viaduct

Figure 1.1 : The Expressway Link (Korea) [2].

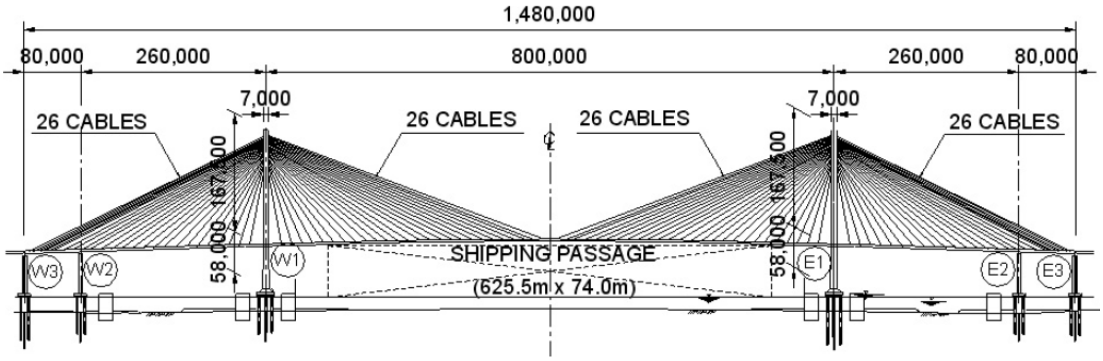
1,480,000
80,000
260,000
800,000
260,000
80,000
7,000
7,000
26 CABLES
26 CABLES
26 CABLES
26 CABLES
167,500
167,500
58,000
58,000
SHIPPING PASSAGE
(625.5m x 74.0m)
W3
W2
W1
E1
E2
E3

Figure 1.2 : Incheon Bridge Elevation [2].

Figure 1.3 : Incheon Bridge (Korea) [2].

1.3 Tatara Bridge, Japan

Tatara Bridge is linking Ikuchijima Island in Hiroshima Prefecture and Ohmishima Island in Ehime Prefecture [4].

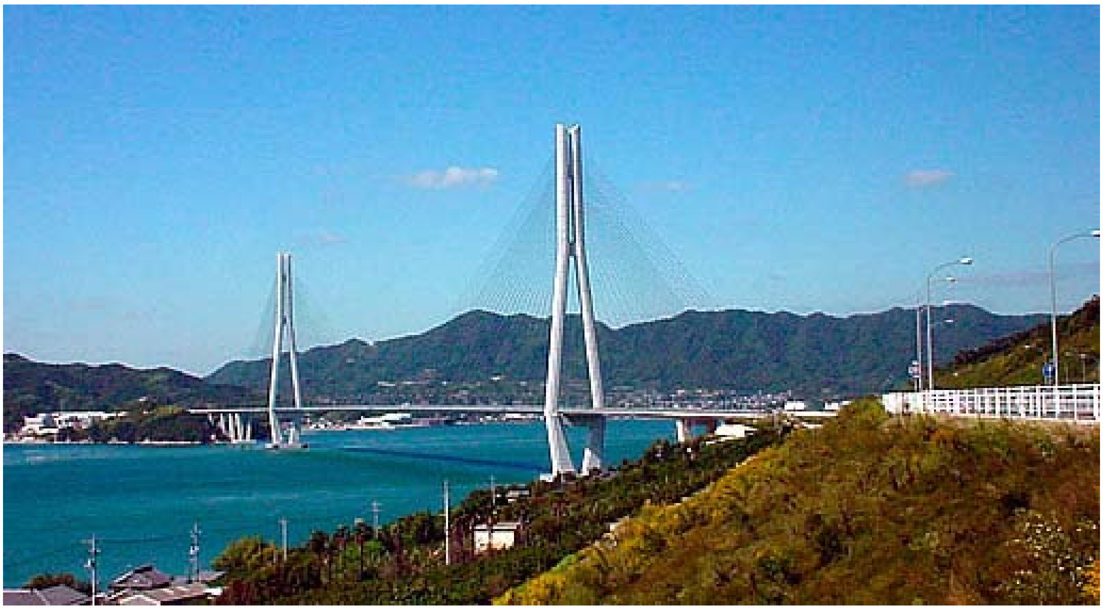

Figure 1.4 : Tatara Bridge (Japan) [4].

Its total lenght is 1480m with 50 + 50 + 170 + 890 + 270 + 50m span lenghts. Main girder is a streamlined orthotropic boz girder. Y shape concrete pylons with semi-fan type cable arrangement was employed [4]. The elevation of the bridge is shown in Figure 1.5.

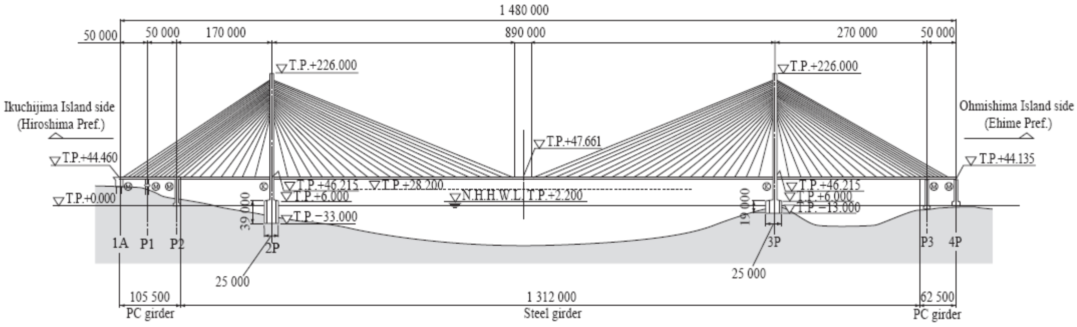
1 480 000
50 000
50 000
170 000
890 000
270 000
50 000
T.P.+226.000
T.P.+226.000
Ikuchijima Island side
(Hiroshima Pref.)
Ohmishima Island side
(Ehime Pref.)
T.P.+47.661
T.P.+44.460
T.P.+44.135
T.P.+46.215
T.P.+28.200
T.P.+6.000
N.H.H.W.L. T.P.+2.200
T.P.+0.000
39 000
T.P.−33.000
T.P.+46.215
T.P.+6.000
19 000
T.P.−13.000
1A
P1
P2
2P
3P
P3
4P
25 000
25 000
105 500
PC girder
1 312 000
Steel girder
62 500
PC girder

(Note) T.P. : Mid-tide in Tokyo Bay (unit : m)
N.H.H.W.L : Nearly highest tide level (unit : m)

Figure 1.5 : Tatara Bridge Elevation [4].

2. CABLE-STAYED BRIDGES CONFIGURATION

2.1 Configuration of Cable Stayed Bridges

In this section the different structural configuration types of cable-stayed bridges and their effect on structural behavior under static and dynamic loads with the long span bridges perspective is given. Since all long span bridge projects are unique, their solutions are unique. Hence, the full understanding and consideration should be provided to choose the best solution for the specific configuration of these cable systems.

2.1.1 General Layout

Cable stayed bridges are three dimensional structures that consist towers, cables, girders. They primarily resist to vertical forces acting on the main girder and also to earthquake and wind induced forces horizontally.

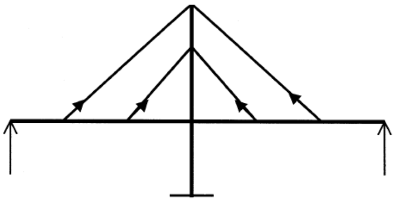

Figure 2.1 : Concept of a cable stayed bridge [5].

From Figure 2.1, it can be inferred that all structure parts are mainly under the effect of axial force. Girders transfer the vertical load to cables and transfer carry them to pylons. Inclination of the cables cause horizontal internal forces which are balanced at the pylon section and axial compression at the girder section.

Three of the longitudinal cable arrangement types are depicted in Figure 2.2.

The anchorage detailing at the top of the pylon for radial arrangement is very complex due to very large vertical axial force on the pylon. However, it is considered as the best structural solution for girder and cables. Because the inclination to the girder of cables are very high and the minimum horizontal component of the loads are carried by the girders. [6]

Harp type arrangement cause bending moments in the pylon but the stiffness of the main girder is improved in comparison with the radial type. [6]

Fan type longitudinal cable arrangement is the combination of other two types and gives the optimum solution for the very long spans.

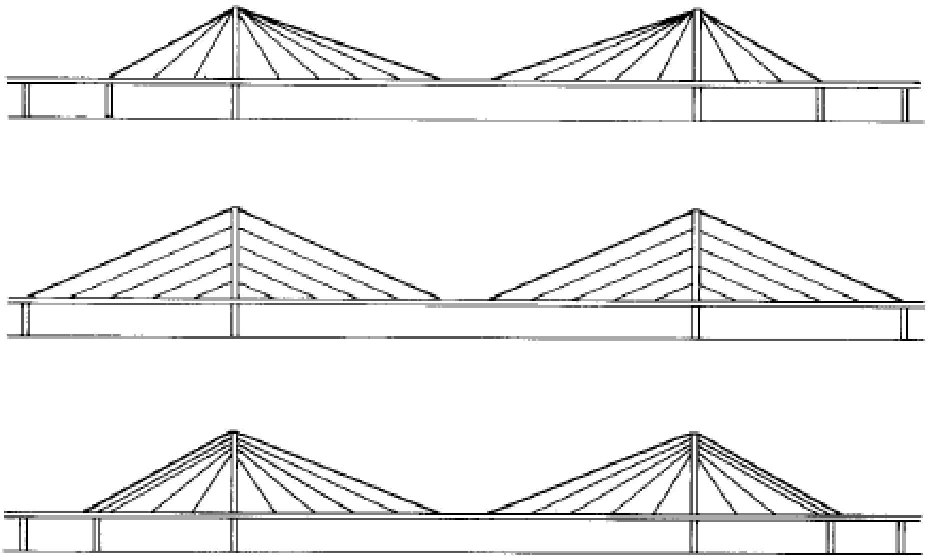

Figure 2.2 : Radial, harp and semi-fan (modified fan) arrangements for cable-stayed bridge systems [7].

It should be noted that the cable arrangement has no significant effect on the bridge structures except very long span bridges.

The superstructure transfers horizontal loads caused by ground motion and wind to both pylons and piers by bending.

2.1.2 Towers and Spatial Cable Layout

Types of arrangements are shown in Figure 2.3. Among these types two inclined plane arrangement is preferable for long span cable stayed bridges because of its torsional rigidity against wind loads.

The role of the towers is to provide support for cables and transfer the loads on bridge to its foundations. They are subjected to high axial forces. Also, bending moment can arise as explained in harp type cable arrangement.

The shape of towers are mainly dependent on the cable arrangemet. H and I type towers allow vertical planes of cables while the A and diamond shape towers provide inclined cable planes.

For single plane system wider girder width is needed because of the position of pylons at the centre of the roadway. In addition, the girder itself has to have the adequate torsional rigidity to resist the eccentric live load loading within the allowable limits. Besides, low fatigue loading on cables is achieved due to the load transferring capability of the rigid girder. Also the second order moments are reduced by the contribution of the rigid girder.

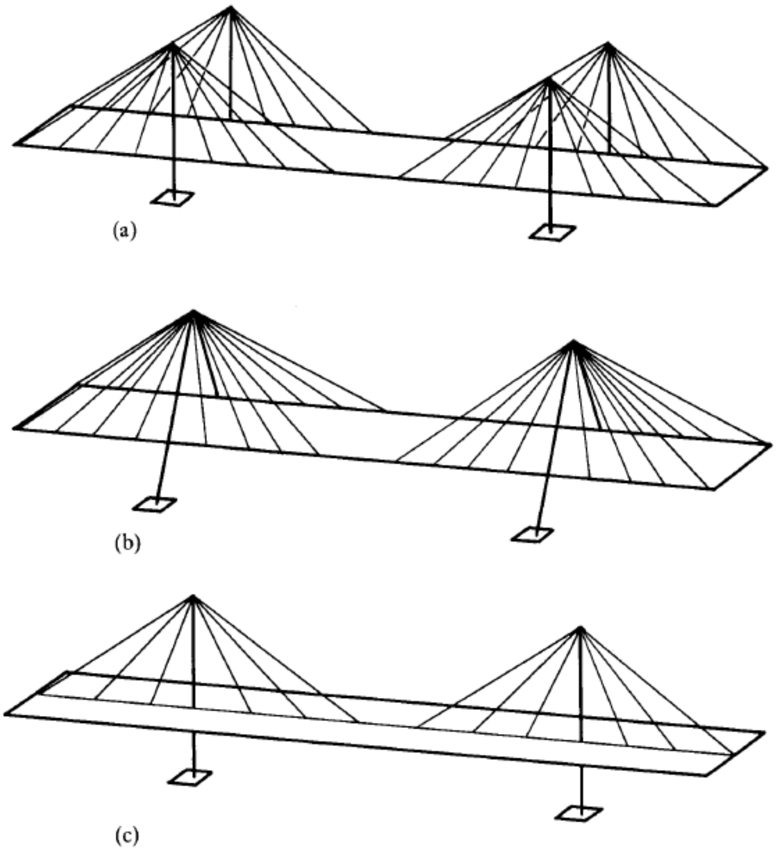

Figure 2.3 : a) Two vertical plane b) Two inclined planes c) Single plane systems[6].

Vertical lateral suspension as in H type pylons provide more rigid links between the girder and the pylon.

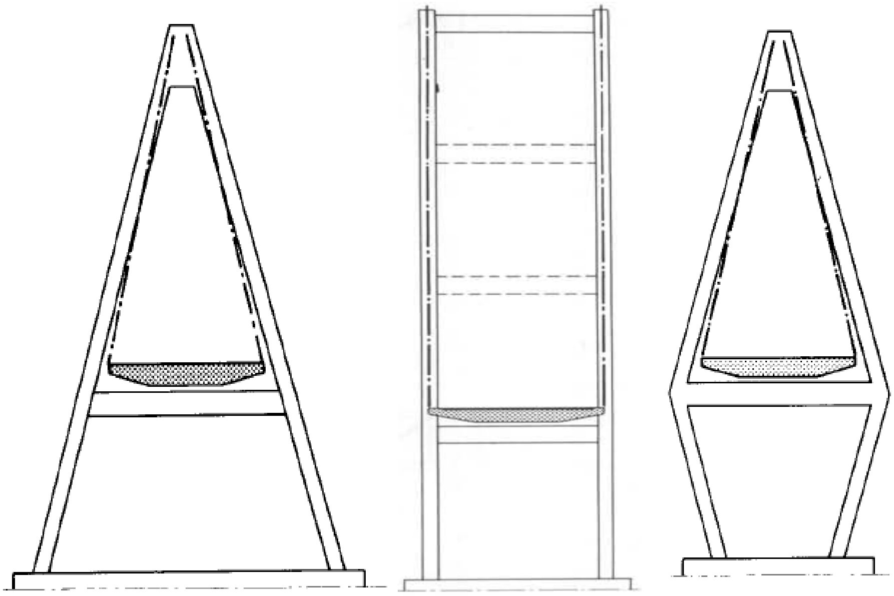

Figure 2.4 : A, H and Diamond configurations of Towers.

A and diamond shaped towers provide better structural stiffness and stability. Under the effect of bending moment the inclined cables and the girder behaves as a closed rigid form. In addition, the rotations deformations are minimized which points out better torsional rigidity in contrast with H and I shape pylons.These type of pylons are especially employed when the aerodynamic effects are a concern as in very long span bridges [8].

2.1.3 Stiffening Girder

The cable system introduces the considerable amount of axial compression forces to the girder. Also, the vertical bending moment arise due to dead load and live load acting on the girder.

The moment of inertia of the girder and the spacing between cables are the controlling parameters of the vertical bending moment.

The girder is supported by cables, which provide longer spans to achieve and minimum internal forces. It can be considered as an elastically supported beam. The global component of this type girder moment is approximately [9]

$$M = a \times p \times \sqrt{I/k} \qquad \textbf{(2.1)}$$

where

a: a coefficient dependent to load type p

I: moment of inertia of the girder

k: elastic support constant derived from the cable stiffness

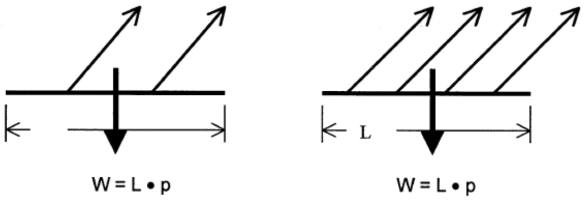

Figure 2.5 : Cable span length – force relation [5].

The relation between the span of cables and force acting on it is given by Figure 2.5. the local bending moment of the girder is dependent to the square of spacing between cables. [5]

According to above given information the smaller spacing between cables provide smaller bending moments and so, slender girder sections.

Slender girder sections are susceptible for buckling phenomenon. However, according to Tang [10].

Cable stiffness is more related to the buckling stability of the girder than the stiffness of the girder itself. The formulation is given in Equation 2.2.

$$P_{cr} = \{\int EIw''^{2}ds + \sum EC \times Ac \times Lc\}/[\int (Ps/Pc)w'^{2}ds] \qquad \textbf{(2.2)}$$

A cable-stayed bridge is still can be stable even if the stiffness of the girder is not considered. Experience shows that even for the most flexible girder, the

critical load against elastic buckling is well over 400% of the actual loads of the bridge [5].

Prestressed concrete, composite, steel I girder are the most used girder types for moderate span lenghts. Orthotropic steel girders are the most adopted type for long span bridges.

2.1.4 Cables and Anchorages

Cables are the main structural elements that transfer the loads from main girder to towers. Development of the stay cable technology leads to the successful long span bridge projects.

Three categories of the cable types; paralel-wire cables, stranded cables and locked coil strands. They are of high strength and have a satisfactory fatigue behavior.

Paralel wires consists of 50 to 350 number of 7 mm diameter wires and they are of high strenght. Each strand consists of seven twisted wires and their quality is widely varied.

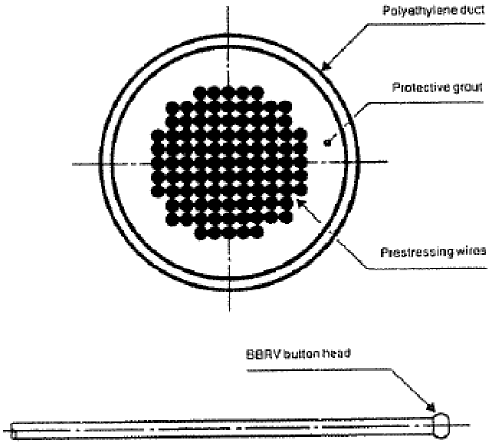

Figure 2.6 : Parallel wire cable [8].

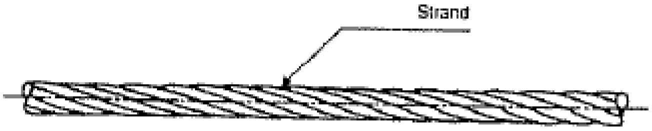

Figure 2.7 : Strand Cable [8].

Locked-coil cable consist a core of parallel wires and S and Z shaped elongated sections which are overlapping outside of the core. Due to their %30 higher density and slimmer sections may be achieved which lead to better aerodynamic behavior. In addition, they are less susceptible to corrosion and their elasticity modulus is about %50 higher than the other types of cables.

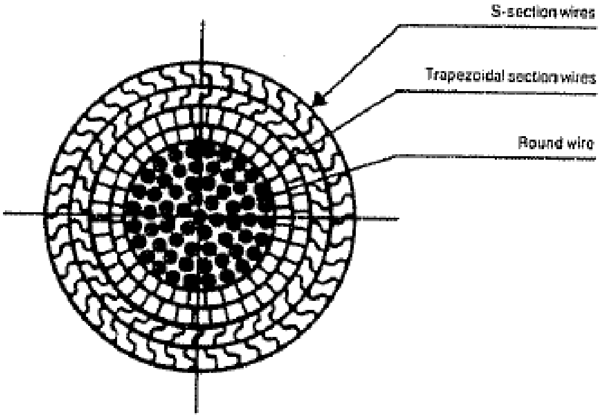

Figure 2.8 : Locked-coil cable [8].

To achieve the allowable stress of cables the capacity and fatigue are should be significantly considered at the the weakest parts of the cables, anchorages.

Three solutions for acnhoring the cables to the concrete pylon is depicted in Figure 2.9. Cables anchored inside of the hollow concrete pylon section in (a) which the forces transffering form the one face to another face of the pylon. In (b) the cable is continous. The horizontal force can be transferred without any effect on pylon. In figure (c) the cables cross through the pylon and mutual bearings sockets can be achieved. Also the axial force arise from the horizontal component of cable. [7]

The torsion caused by the eccentric overlapping of cables (Figure 2.10 a) can be avoided by the use of a detail shown in Figure 2.10 (b).

Fixed supports at the pylon may be provided by devices like pin or socket and movable supports are provided by roller or rocker.

The configuration of deck anchorages depend on the type of cable used. Special threaded sockets are used for connection and bolts are used to adjust the pretension on cables. Further information can be found in literature [6], [7], [8], [11].

level.

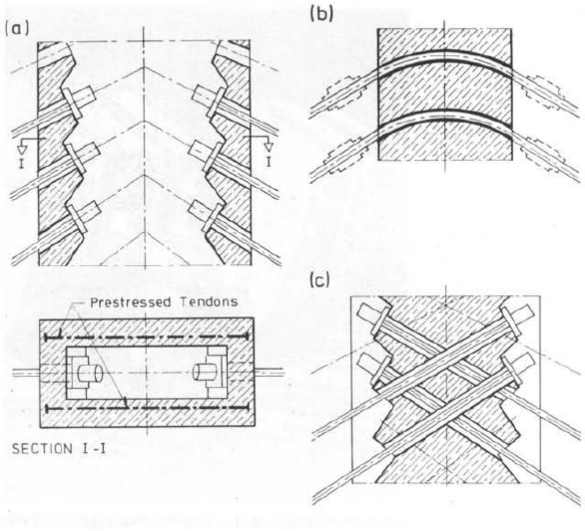
(a)
(b)
I
I
(c)
Prestressed Tendons
SECTION I -I

Figure 2.9 : anchoring of mono-strand cables to a concrete pylon [7].

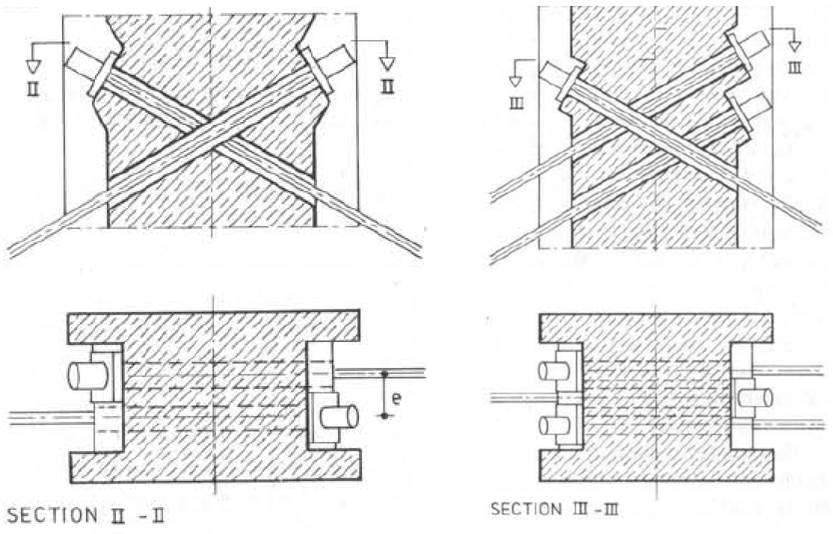
II
II
III
III
e
SECTION II - II
SECTION III - III

(a) **(b)**

Figure 2.10 : Overlapping of stay cable anchorages with and without eccentricity[7].

2.1.5 Foundations

Foundations are the structural elements where the loads acting on bridge is tranferred to ground. Pile foundations are the most utilized type of foundation for cable stayed bridges. Also caissons are employed when the foundation is at the sea level.

3. STATE OF THE RESEARCH ON CABLE-STAYED BRIDGES

3.1 Nonlinearities in Cable Stayed Bridges

Nonlinearities in cable-stayed bridges are identified by many investigators [12], [13], [14], [15]. These are;

a) cable sag effect

b) Axial force and moment interaction in pylons and girders

c) The effect of relatively large deformations of whole system due to its flexibility – P-Δ effects.

d) Material nonlinearity

Cable weight itself lead to sagging of a cable to a catenary shape, and the external tension force results in a reduction of this out of plane deformation. Hence, the actual stiffness of cable varies with the applied tension force and the total weight of the cable as well as its cross-sectional area and inclination angle. Ernst has been the first who explain this stiffness change with a nonlinear formulation [16].

$$E_{eq} = \frac{E_0}{1+\frac{\gamma^2 \times L^2 \times E_0}{12 \times \sigma^3}} \qquad \textbf{(3.1)}$$

Formulation given in Eq. (3.1) represents the tangential value of the equivalent modulus of elasticity when stress on the cable is equal to σ.

If the stress on cable is changing form an inital value of σ_i to a final value of σ_f during an incremental loading, then the equivalent modulus of elasticity, which represents the secantial value, is given by Eq (3.2).

$$E_{eq} = \frac{E_0}{1+\frac{\gamma^2 \times L^2 \times \left(\sigma_i+\sigma_f\right) E_0}{24 \times \sigma_i^2 \times \sigma_f^2}} \qquad \textbf{(3.2)}$$

The stress-strain relationships in cases of tangential and secantial values of E_{eq} are depicted in Figure 2.1.

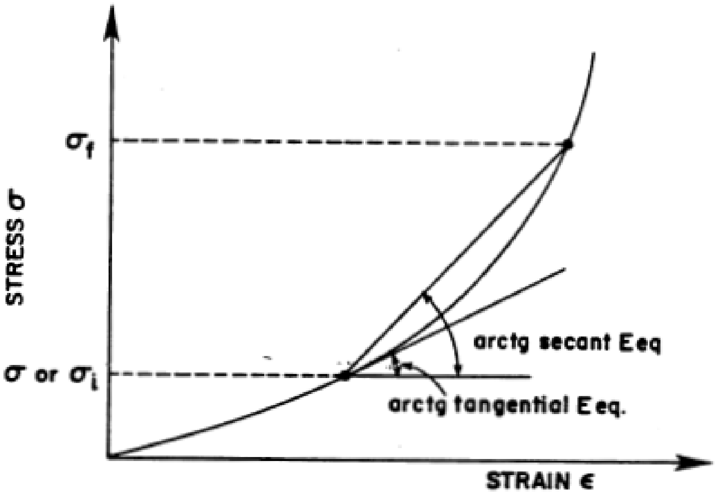

Figure 3.1 : Nonlinear stress-strain relationship for a cable-stay [1].

Equivalent modulus of elasticity should be defined by using the cable pretresses resulting from the nonlinear dead load analysis of the structure for accurate results in dynamic analysis [13].

Since equivalent elasticity modulus approach is suggesting the stiffness of the structure is increasing as tension forces increase, cable-stayed bridges are defined as geometric-hardening type of structure. This behaviour is depicted in Figure 3.2 [17], [18], [19].

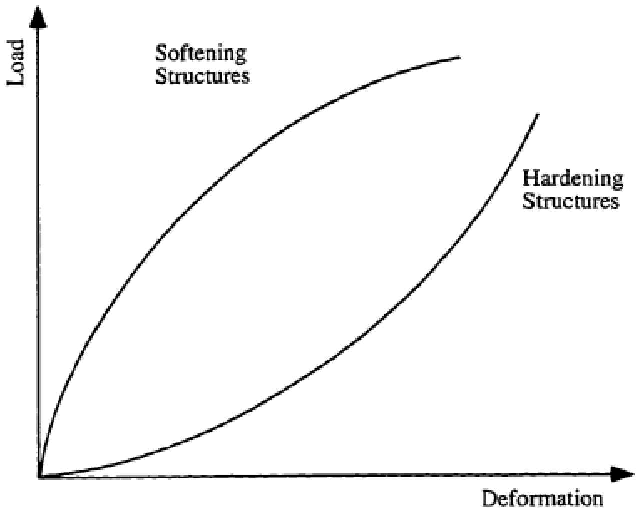

Figure 3.2 : Geometric hardening type (adapted from [17]).

Nonlinear behaviour of bending members, towers and girders, caused by interaction of axial and bending forces. [13] Flexural and axial stiffnesses of the members alter under these combined effects and these nonlinear element formulations can be found in [20].

The stiffness matrix of the structure should be updated due to deformed state of these flexible bridges to represent the relatively large geometry changes in overall structure [14], [15].

Material nonlinearity is not considered in this study. Information on this subject can be found in literature.

2.2 Dynamic Characteristics and Response

Two major dynamic loads, aerodynamic and seismic, are in contradict when their demands on structure is considered. Stiffer structures are better for stability of the aerodynamic behavior and it is a well known fact that the seismic response will have less demand when more flexible structure is considered.

It is essential to obtain natural periods, natural mode shapes and damping characteristics accurately in seismic and aerodynamic analysis and design of cable-stayed bridges.

3D modelling is mandatory to obtain reasonable and accurate results, since Abdel-ghaffar and Nazmy found that there were significant coupling of modes in the three orthogonal directions [1], [21].

Supporting conditions of the structure is an important consideration which affects the dynamic response of the structure. Nazmy and Abdel-Ghaffar [22] investigated the mode distribution depending on support conditions. The bridge with movable supports have the longest period due to higher flexibility. Servicability limits should also be taken into account to choose the supporting conditions.

Many full scale tests and numerical analysis were conducted to obtain accurate mode shapes and natural frequencies of cable-stayed bridges. From these researches it can be said that the linear analysis that assume appropriate mass and stiffness properties distribution is capable of obtaining these results. [23] Eigen value analysis were carried out to understand the dynamic response characteristics of cable-stayed bridges by many researchers which will be given in this section. Many researchers stated that the fundamental period of a cable-stayed bridge is very long compared with other structures. First modes are usually deck modes, followed by coupled cable and deck modes and coupled tower and deck modes [18].

Most of the excitation test were conducted by means of vertical flexural and torsional ocsilaions to verify the aerodynamic stability of the cable-stayed bridges. Kawashima and his co-workers were conducted several excitation tests on Meiko-nishi Bridge not only for vertical flexural ocsillations but also for transverse flexural oscilations which are as important as the vertical flexural and torsional oscillations. The cable arrangement is fan type and the deck is a steel box girder. Obtained frequencies from the excitation tests are depicted in Table 3.1 [24].

Table 3.1 : Natural Frequcies of Meiko-nishi Bridge (adapted from [24]).

	Vertical Flexural	Torsion	Transverse Flexure
1st	0.33	1.31	0.26
2nd	0.41		0.71
3rd	0.73		0.76
4th	0.81		1.01
5th	0.85		

Daniell and MacDonald also conducted series of ambient vibration tests, among other issues, to verify the natural frequencies which are computed by linear and geometric nonlinear analysis procedures [25]. These values are depicted in Figure 3.3.

It is essential to perform a nonlinear dynamic analysis for spans longer than 450 m [13]. For spans up to 450 m a linear dynamic analysis may be adequate to obtain peak structural responses, but it must be preceeded by a nonlinear dead load analysis.

Linear and nonlinear analyses were also investigated by abdel-ghaffar [18] and three analysis methods, which are explained below, were compared for dynamic anaylsis of two bridges with center span lenghts 335 m (1100 ft) and 670 m (2200 ft).

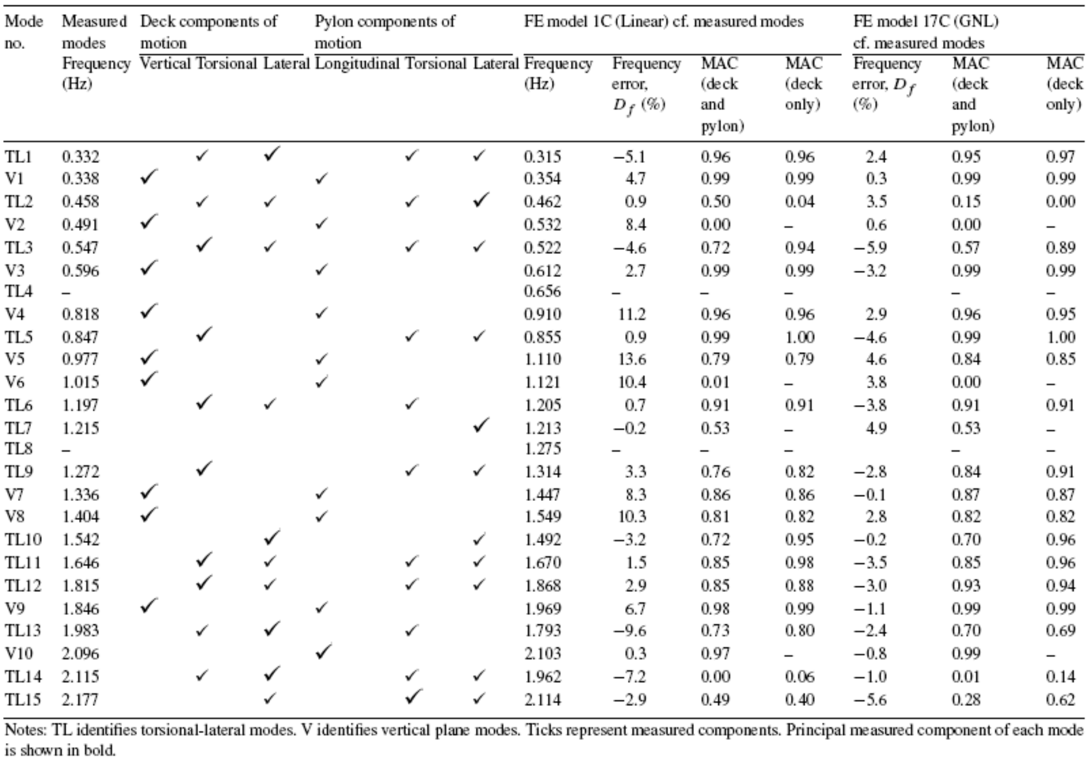

Mode no.	Measured modes	Deck components of motion			Pylon components of motion			FE model 1C (Linear) cf. measured modes				FE model 17C (GNL) cf. measured modes		
	Frequency (Hz)	Vertical	Torsional	Lateral	Longitudinal	Torsional	Lateral	Frequency (Hz)	Frequency error, D_f (%)	MAC (deck and pylon)	MAC (deck only)	Frequency error, D_f (%)	MAC (deck and pylon)	MAC (deck only)
TL1	0.332		✓	**✓**		✓	✓	0.315	−5.1	0.96	0.96	2.4	0.95	0.97
V1	0.338	**✓**			✓			0.354	4.7	0.99	0.99	0.3	0.99	0.99
TL2	0.458		✓	✓		✓	**✓**	0.462	0.9	0.50	0.04	3.5	0.15	0.00
V2	0.491	**✓**			✓			0.532	8.4	0.00	–	0.6	0.00	–
TL3	0.547		**✓**	✓		✓	✓	0.522	−4.6	0.72	0.94	−5.9	0.57	0.89
V3	0.596	**✓**			✓			0.612	2.7	0.99	0.99	−3.2	0.99	0.99
TL4	–							0.656	–	–	–		–	–
V4	0.818	**✓**			✓			0.910	11.2	0.96	0.96	2.9	0.96	0.95
TL5	0.847		**✓**			✓	✓	0.855	0.9	0.99	1.00	−4.6	0.99	1.00
V5	0.977	**✓**			✓			1.110	13.6	0.79	0.79	4.6	0.84	0.85
V6	1.015	**✓**			✓			1.121	10.4	0.01	–	3.8	0.00	–
TL6	1.197		**✓**	✓		✓		1.205	0.7	0.91	0.91	−3.8	0.91	0.91
TL7	1.215						**✓**	1.213	−0.2	0.53	–	4.9	0.53	–
TL8	–							1.275	–	–	–		–	–
TL9	1.272		**✓**			✓	✓	1.314	3.3	0.76	0.82	−2.8	0.84	0.91
V7	1.336	**✓**			✓			1.447	8.3	0.86	0.86	−0.1	0.87	0.87
V8	1.404	**✓**			✓			1.549	10.3	0.81	0.82	2.8	0.82	0.82
TL10	1.542			**✓**			✓	1.492	−3.2	0.72	0.95	−0.2	0.70	0.96
TL11	1.646		**✓**	✓		✓	✓	1.670	1.5	0.85	0.98	−3.5	0.85	0.96
TL12	1.815		**✓**	✓		✓	✓	1.868	2.9	0.85	0.88	−3.0	0.93	0.94
V9	1.846	**✓**			✓			1.969	6.7	0.98	0.99	−1.1	0.99	0.99
TL13	1.983		✓	**✓**		✓		1.793	−9.6	0.73	0.80	−2.4	0.70	0.69
V10	2.096				**✓**			2.103	0.3	0.97	–	−0.8	0.99	–
TL14	2.115		✓	**✓**		✓	✓	1.962	−7.2	0.00	0.06	−1.0	0.01	0.14
TL15	2.177			✓		**✓**	✓	2.114	−2.9	0.49	0.40	−5.6	0.28	0.62

Notes: TL identifies torsional-lateral modes. V identifies vertical plane modes. Ticks represent measured components. Principal measured component of each mode is shown in bold.

Figure 3.3 : Correspondence between modes from ambient vibration tests and from FE model 1C (linear analysis) and 17C (Geometric Nonlinear Analysis) [25].

L-L: Linear static analysis followed by linear earthquake analysis

NL-L: Nonlinear static analysis followed by linear earthquake analysis

NL-NL: Nonlinear static analysis followed by nonlinear earthquake analysis

Results suggested that for structure with 335 m center span (model 1), response difference between the NL-L case and NL-NL case is small. However, L-L case was considerably differ from the other two in response manner. The response characteristics are depicted in Figure 3.4.

For the model with 670 m center span at the same study the nonlinear dynamic analysis response was found more pronounced than model 1. Hence, geometric, as well as general nonlinear dynamic analysis is necessary for calculating the response of long span bridges subjected to strong ground excitation.

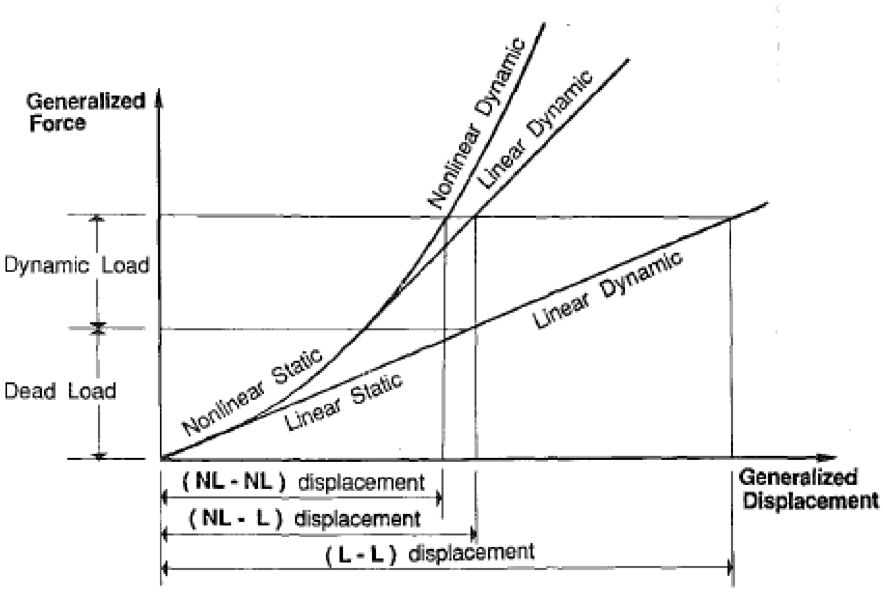

Figure 3.4 : Response comparison between linear and nonlinear analysis[18].

Multi support excitations should also be carried out in dynamic analysis of long span bridges to take into account the spatial variability of the ground motion on the structural response. They can have a significant effect on the response displacements and member forces and these response quantities may be substantially increased by non uniform ground motion [18], [26]. The authors also stated that at least three diffrent types of ground motions consistent with the location of the bridge should be considered in the calculation of the time history response to make realistic seismic design.

Response characteristics under the effect of vertical component of ground motions will be discussed in detail in Section 4.4.

3.3 Damping Characteristics

Cable-stayed bridges have inherently low values of damping and it is difficult to generalize damping values because it varies significantly with the bridge configuration as demonstrated by many field-forced vibration tests.

Kawashima stated that damping ratio of cable-stayed bridges is predominantly dependent on material nonlinearity, structural damping mechanisms, radiation of energy from foundation to ground and friction with air [27]

Fleming & Egeseli stated that the damping can have significant effect upon the response of the bridge structures and should be considered and realistic values of damping should be investigated for further analysis [13].

Two ways to consider damping in the analysis. First, material nonlinearity and special energy dissipation devices may be included in the analysis with nonlinear, elastic-plastic, hysteretic modeling of the elements. However, most commonly, although the damping in cable-stayed bridges is not viscous; an equivalent viscous damping can be utilized in the analysis. Rayleigh damping, which is a linear combination of mass and stiffness matrix, is empoyed to form damping matrix. It enables satisfying damping ratio exactly for 2 modes [28]. Damping ratios of 2-3% have been employed by many researchers [29], [30].

Extensive experiments are carried out by Kawashima and his co-workers [27], [31], [32]. A cable-stayed bridge is analysed with strong motion records and it was found that the damping ratio is dependent on the mode shapes in [33] . For further research, an analytical approach which consider several substructures to evaluate the damping ration is adopted by Kawashima et al. in [27]. These could be cables, deck, bearing supports and etc. The summation of the energy dissipation of each individual substructure result in the total energy dissipation of the bridge structure. An experimental model of Meiko-nishi Bridge, depicted in Figure 3.5, was fabricated and model oscillation tests were made. Cable arrangement, amplitude of oscillation and the mode shapes are the most significant factors that effect the damping values. Damping values predicted by the derived enery dissipation functions and the experimantal results are compared in [27]. These comparisons are depicted in figures 3.6 and 3.7.

Kawashima et al. [33] also investigated the damping values under the effect of real strong motion excitation. Results suggested that the values were higher than values resulted from forced vibration tests. %2 and 0-1% in both directions for towers and %5 in both directions for deck are obtained when the strong ground motion was considered.

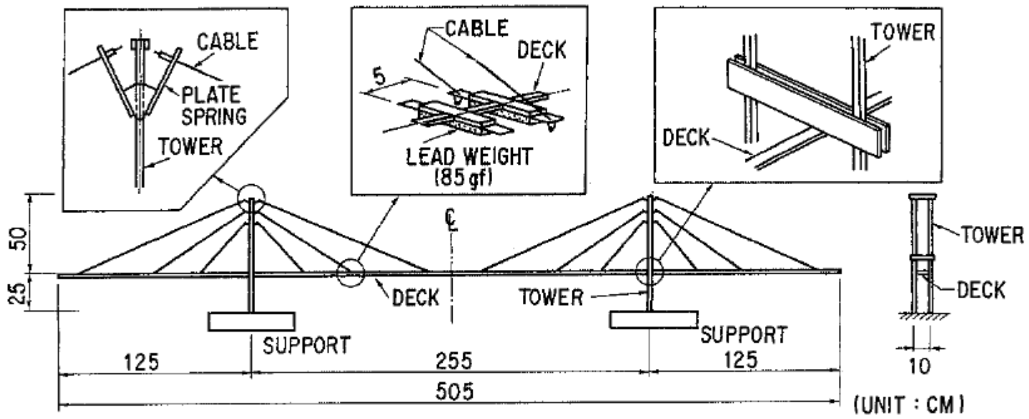
CABLE
PLATE SPRING
TOWER
CABLE
DECK
5
LEAD WEIGHT (85 gf)
TOWER
DECK
50
25
℄
DECK
TOWER
SUPPORT
SUPPORT
125
255
125
505
TOWER
DECK
10
(UNIT : CM)

Figure 3.5 : Meiko-nishi Bridge experiment model [27].

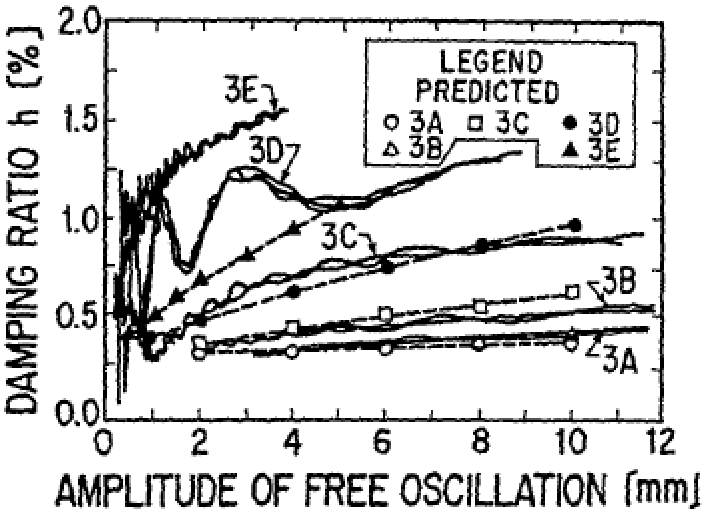

Figure 3.6 : Comparison of damping ratio versus oscillation amplitude relation for longitudinal oscillation [27].

Wilson et al. [34] obtained %2-2.6 and %0.9-1.8 upper and lower bound damping ratio values of Quincy Bayview Bridge were obtained for the first coupled transverse/torsion mode.

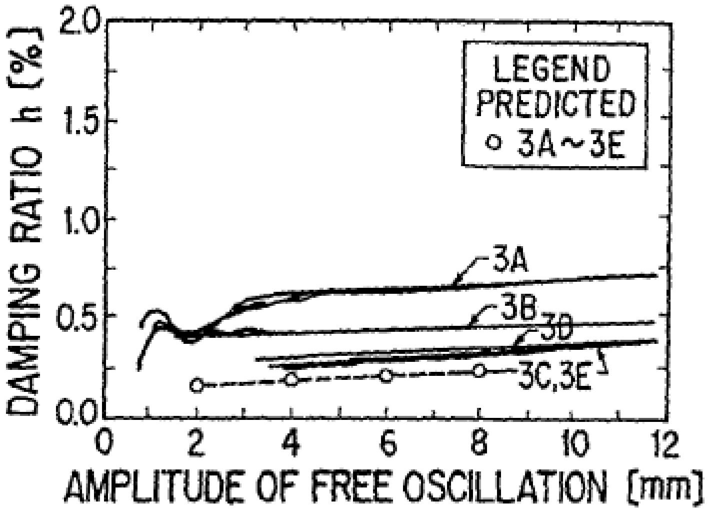

Figure 3.7 : Comparison of damping ratio versus oscillation amplitude relation for vertical oscillation [27].

4. BRIDGE CONFIGURATION

4.1 Structure Description

The bridge considered in this study is a hypothetical example which reflects the contemporary trend of long span cable-stayed bridges. The choice of structural properties of the elements in the mathematical model was based on examining several recently constructed long span cable-stayed bridges. [2], [3], [4].

A cable stayed bridge with the span arrangements 100+250+700+250+100, which will be named as IY 700 here after, is considered to represent the current trend of long span bridge projects. The preliminary analysis is carried out and design limit states are checked. These calculation results will be given in Chapter 5.

Vertical profile of the bridge consists of a precamber with %1.5 vertical slope, to compensate the dead and live load deflections. Also counterweights are arranged in the back spans to resist uplift forces in the mid piers. Semi-fan arrangement of cables is adopted. The general dimensions of IY 700 are depicted in Figure 4.1.

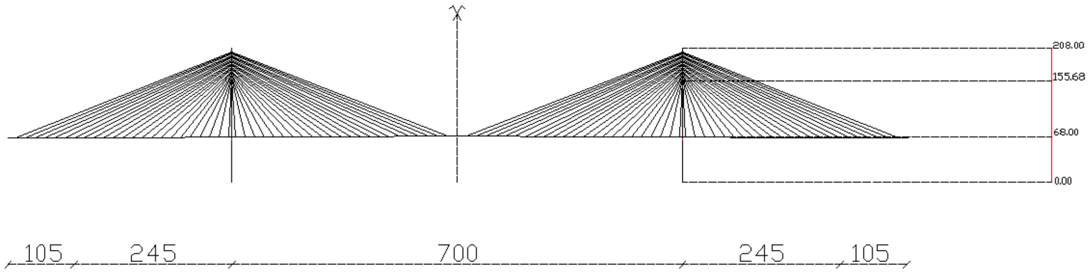

Figure 4.1 : Elevation of IY 700 Bridge.

Material Properties Table for the structural components is shown in Table 4.1.

Table 4.1 : Material properties

	Material	σ_y (Mpa)	$\sigma_{ult.}$ (Mpa)	E (GPa)	Weigth Density (kN/m^3)	Poisson's Ratio
Deck	A572 Gr. 50	345	450	210	77.09	0.30
Cable	ASTM	-	1770	210	77.09	0.30
Pylon	C70	-	-	37	23.50	0.20
Cross Beam	C70	-	-	37	23.50	0.20

4.1.1 The Deck

As mentioned in Section 3.1.3, orthotropic steel box girders are preferable because of their lightweight, torsional rigidity and streamlined cross section shapes. The box girder is 14 m wide by 3 m deep and the central span is 700 m. The deck considered in this study is depicted in Figure 4.2.

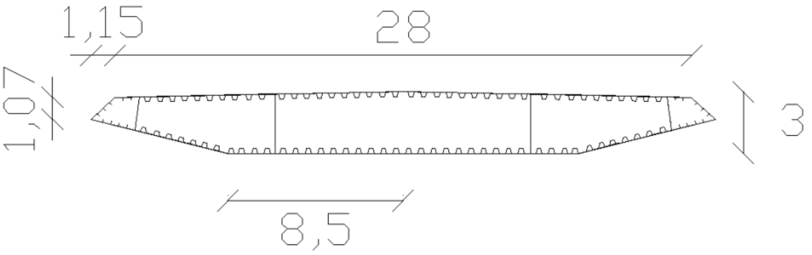

Figure 4.2 : Section of orthotropic steel box girder.

The proportions of the streamlined deck shape are decided based upon the given experimental results by various authors [6], [7], [8], [11].

The torsional moments and lateral forces from box to the bearings are transferred by provided external diaphragms at end and internal supports with a 1.875 m spacing. Intermediate internal plate diaphragms are provided with 3.75 m spacing to ensure the sufficient torsional rigidity and continuity of the stiffening girder. All diaphragms are fully connected to top and bottom flanges and also webs.

Both inner and outer webs are adequately stiffened longitudinally. Access holes within the diaphragms are not taken into consideration.

Since standardization of ribs is not available in AASHTO, the table provided by an American steel company is used. [5]

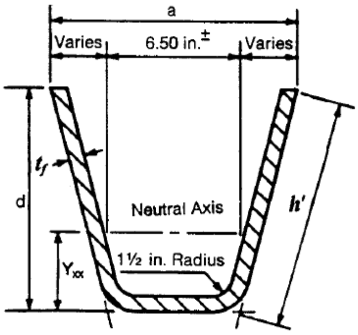

Figure 4.3 : Section of ribs.

Table 4.2 : Rib cross-section properties

a (cm)	d (cm)	t_f (cm)	h' (cm)	Y_{xx} (cm)	I_{xx} (cm^4)
30.79	22.86	1.1	23.95	9.17	3612.9

Stiffening ribs are continous along the bridge. The deck plate is acting as the common flange of both longitudinal ribs, diaphragms and webs.

Wheel load distribution on deck plate is calculated according to AASHTO-LRFD [35]. The tire contact area is calculated as in Article 3.6.1.2.5.

Main girders of the steel orthotropic decks have been modelled either by using equivalent beam elements or complete shell model and also by specific box girder element formulations.

Equivalent beam element models consist beam elements with the actual stiffness properties of the actual girder and fictitious rigid link elements are extended to cable anchorage points which are eccentric to longitudinal center axis of the girder. This model is named as “spine beam” and used effectively in many studies.

Complete shell model and specific box girder element formulation are the other options to model girder which they could result in more accurate response characteristics.

4.1.2 The Pylons and Piers

Diamond shape pylons are employed to improve the overall torsional stiffness of the structure. The pylons are 208 m high with a 140 m height above the main span deck elevation.

Beam elements are utilized to model the pylons, and piers are respresented by supports. Solid elements may be used for more refined analysis to consider the shear force effects accurately. These effects are not taken into account in this study for simplicity.

4.1.3 The Stay Cables

Two inclined stay cable plane arrangement is of semi-fan type which is utilized. There are total 184 units of cable with 92 units per each side. Cable spacing is small in comparison with the length of the spans due to the considerations explained in Section 3.1.3. The longest stay cable is about 360 m with an approximate weight of 300 kN.

Material properties of cables given in Table 4.1 are adopted from the VSL International, Ltd. brochure to reflect the modern trend of the stay cable technology. Parallel wire stand consisting of 7 mm diameter strands, each with a cross sectional area of 38.48 mm^2 is adopted for the analysis. Cables sizes range from a maximum of 0.0154 m^2 for the back span cable to a minimum of 0.0054 m^2 for the cables near the pylons.

One straight chord truss element may be used to represent each cable only if the equivalent elasticity modulus approach is utilized. Tangential modulus obtained as explained in Section 3 is used for computing the tangent stiffness matrix of the stay cable.

Multi element model is another option to represent cables to investigate the cable vibration and its interaction with deck and tower modes which is not considered in this study.

5. FINITE ELEMENT MODEL OF THE BRIDGE

5.1 Introduction

3D finite element model of IY 700 was set up with COSMOS-M [36] for the purposes of static and dynamic analysis and it is depicted in Figure 5.1. In this chapter, properties of the structural model of the bridge and assumptions made are given in detail.

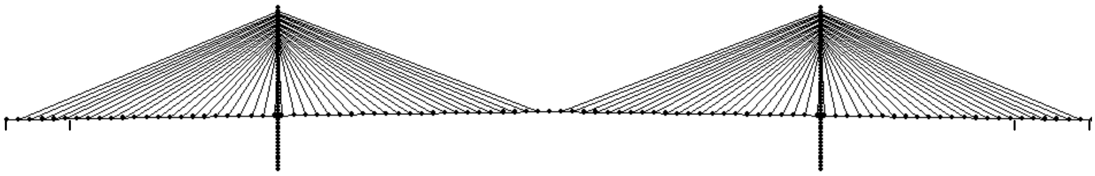

Figure 5.1 : Finite element model of the bridge.

5.2 Description of the finite element model

5.2.1 The deck

Since the dynamic behaviour of the bridge is considered, it is important to set up a model to simulate the coupling of modes in the three orthogonal directions accurately. Hence, 3D analysis is necessary [21].

The modelling approach given by Wilson and Gravelle [37], is adapted to model the deck. The model consist a linear elastic beam elements which form the single central spine and rigid links extending to the cable anchor and lumped mass points of the deck. Mechanical properties of the equivalent beam is calculated by establishing an exact cross section of the girder. The cross section is uniform along the bridge.

Also, a model which consist the exact shell representation of the girder to check the accuracy of the equivalent beam model under static load conditions. Since the two models are in good accordance by all means of deflections, moment distribution etc., the equivalent beam model is used for the rest of the analysis. The mechanical properties of the cross section is depicted in Table 5.1.

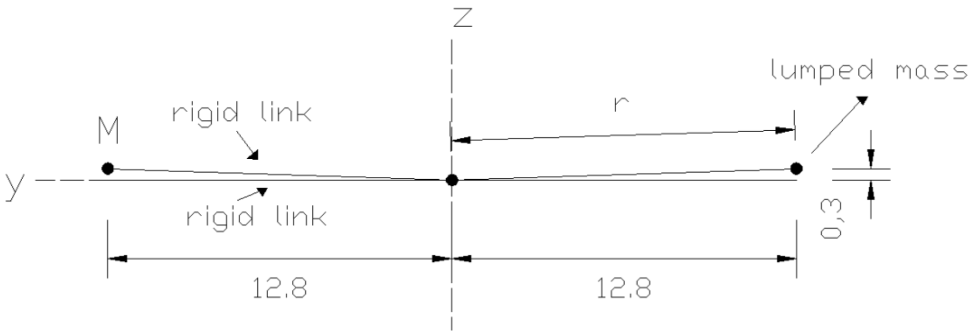

Figure 5.2 : Finite element modelling of the cross section of the deck.

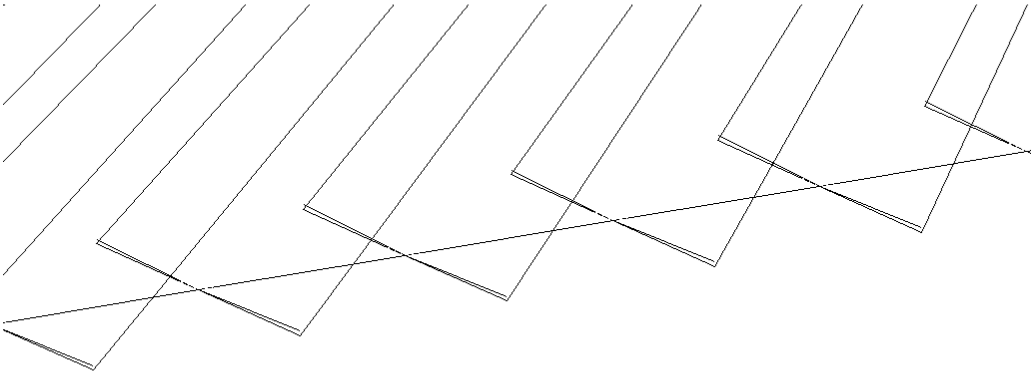

Figure 5.3 : Finite element model of the deck.

The finite element model of the deck is depicted in Figure 5.3. The spine has 96 beam elements spanning between the cable anchor points and the supports with a 15 m or 5 m intervals along the longitudinal (x) direction of the bridge.

Table 5.1 : Stiffness properties of the box girder

A (m^2)	I_y (m^4)	I_z (m^4)	I_{yz} (m^4)
2.21	2.63E+00	1.37E+02	9.70E+00

Equivalent plate thickness of the ribs is taken into account to calculate the vertical (I_y), transverse (I_z) and torsional stiffness (I_{yz}) properties. Both pure and warping torsional stiffnesses are taken into account to calculate the overall torsional stiffness of the cross section.

The mass of the deck consist both contribution from the cross section and the mass of the utilities assumed distributed along the bridge. The weight properties are depicted in Table 5.2.

Table 5.2 : Weight properties of the deck

Back Span (kN/m)	Side Span (kN/m)	Main Span (kN/m)
189.08	169.08	169.08

Translational mass is calculated from the total weight of each segment either 15 m or 5 m including the contributions from ribs, plates, webs, and utilities assumed distributed along the bridge. Total mass is divided into three concentrated masses and allocated equally to the spine itself and points of rigid link extensions as can be seen from Figure 5.2.

The distance between the shear center and the neutral axis of bending is taken into account in the finite element model to allow torsional and coupled modes of vibration.

The shear center of the cross section is 0.30 m below the centroid of the bridge which is taken as the vertical distance between rigid links. In the finite element model the spine is placed at the elevation of the roadway and at the shear center. Hence the masses are placed 0.30 m above the spine and also the rotational mass properties are calculated with the contributions of this assumption. The distance between the center of rigidity and center of mass allows producing the coupling between the torsional and transverse modes.

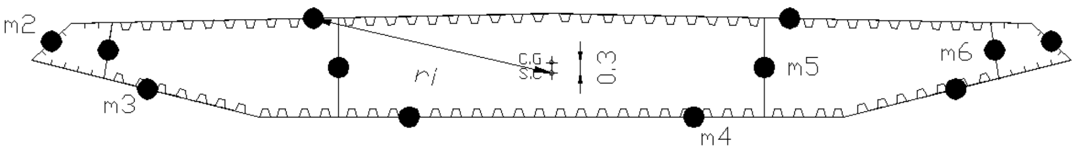

Figure 5.4 : Distribution of lumped masses used in calculating the total lumped masses.

Table 5.3 : Distances between the distributed lumped masses and the shear centre

	r_i (m.)
m_1	7.19
m_2	14.60
m_3	11.78
m_4	4.29
m_5	6.20
m_6	12.93

The mass moments of inertia are calculated using the formula

$$I_{Mi} = \Sigma(I_{mi} + m_i r_i^2) \tag{5.1}$$

where;

I_{mi}: mass moment of inertia of the *i*th element about its own centroidal axis

m: mass of *i*th element

r_i: distance from centre of mass of *i*th element to the shear centre as depicted in Figure 5.4.

The mass moment of inertia of the elements about their own centroidal axis are calculated with the formulation given for plate elements (Eq. 5.3) and rod elements (Eq. 5.4) where necessary.

$$I_{mi}: \frac{m_i}{12} \times \left(L_x^2 + L_y^2\right) \tag{5.2}$$

$$I_{mi}: \frac{m_i}{12} \times \left(L_y^2\right) \tag{5.3}$$

Calculated mass properties are corrected to represent the actual mass moments of inertia in the spine model as indicated in Wilson and Gravelle [37]. These corrected values of translational and rotational mass are depicted in Table 5.4.

Table 5.4 : Mass properties of the deck

Mass Properties		15 m segment	7.5 m segment	12.5 m segment
Translational masses		(kN/g)	(kN/g)	(kN/g)
Main Span		87.78	-	81.40
Side Span		87.78	-	81.40
Back Span		97.97	50.51961575	-
Rotational Inertia		(kN/g x m^2)	(kN/g x m^2)	(kN/g x m^2)
Main Span	I_{Mx}	26641.92	-	17305.14
	I_{My}	8991.99	-	4379.50
	I_{Mx}	23273.65	-	15304.73
Side Span	I_{Mx}	26641.92	-	17305.14
	I_{My}	8991.99	-	4379.50
	I_{Mx}	23273.65	-	15304.73
Back Span	I_{Mx}	29984.03	12902.98	-
	I_{My}	12334.10	5028.46	-
	I_{Mx}	26615.76	12405.81	-

5.2.2 The Cables

The sectional properties and the arrangement of the cable planes are given in Section 4. One truss element is utilized to model each cable with the equivalent elasticity modulus approach. The tangential stiffness matrix is calculated by means of nonlinear dead load analysis and the required cable pretension forces are obtained depending on this analysis. The force – displacement relationship of cables is depicted in Figure 5.5 and the calculated equivalent modulus of elasticity is given in Table 5.5.

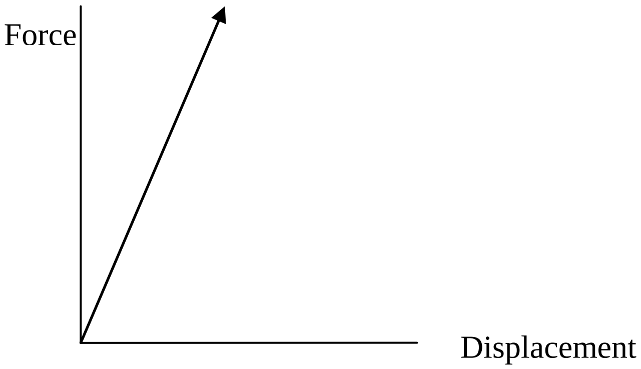

Figure 5.5 : Force – displacement relationship of cables.

Table 5.5 : The calculated equivalent modulus of elasticity of the cables

Cable Group	E (kN/m^2)
1	1,55E+08
2	1,46E+08
3	1,71E+08
4	1,74E+08
5	1,84E+08
6	1,94E+08
7	1,79E+08
8	1,71E+08
9	1,60E+08
Ave.	1,70E+08

5.2.3 The Pylons and Piers

Beam elements are used to model pylons and finite element model of a pylon is depicted in Figure 5.6. Intermediate and end piers are represented as supports since the behaviour of these components is not a concern for this study.

5.2.4 The foundations

The interaction between soil and the structure is not taken into account.

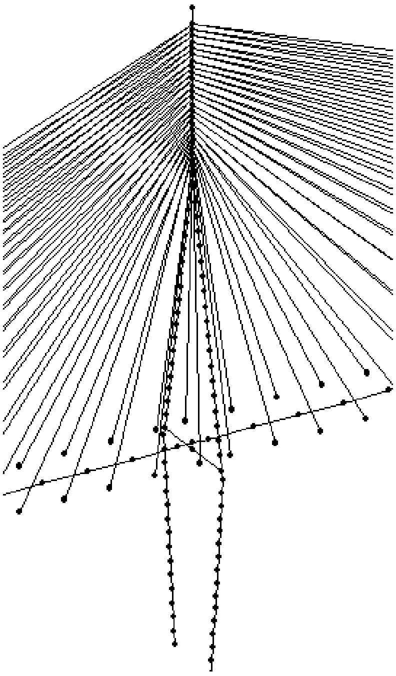

Figure 5.6 : Finite element model of a pylon.

5.3 Static Loading Conditions

The loading conditions which are considered in this study are given in Table 5.6.

Table 5.6 : Loading Conditions

Load	
DC	dead load of structural components and non-structural attachments
DW	dead load of wearing surfaces and utilities
PS	Cable prestress
LL	vehicular live load
IM	vehicular dynamic load allowance
EQ	earthquake

Load factors considered are given in Table 5.7.

Table 5.7 : Load Combinations and load factors

Limit State	DC DD	LL IM	EQ
STRENGTH I	γ_p	1.75	
STRENGTH II	γ_p	1.35	
EXTREME I	γ_p	γEQ	1
SERVICE II	1	1.3	

Table 5.8 : Load factors for permanent loads, γ_p

Type of Load	Maximum	Minimum
DC: Component and Attachements	1.25	0.90
DW: Wearing Surfaces and Utilities	1.5	0.65

5.3.1 Optimization of Cable Pretension

There are infinite number of combinations concerning the pretension forces of any cable stayed bridge. Obtaining the adequate and effective initial shape and internal forces is the most significant task in the analysis of cable-stayed bridges since the structure’s behaviour is dependent to it.

Although it is a well known fact that some of the cable pretension forces may differ from the final form during the construction stage, in this study the final form of the bridge is considered for the optimization process.

Three commonly used methods for obtaining the cable pretension forces have been proposed to adjust the internal force and displacement conditions of cable-stayed bridges. These methods are;

1. Optimization method
2. Zero displacement method
3. Force equilibrium method

Optimization Method

There are many factors that affect the volume/cost and the safety of the structure related to optimization process. Optimization method utilizes objective functions to reach the ideal state of the bridge structure concerning the economy and the safety. Deflection limits, material allowable stresses and the cost of the structure are the primary objective function variables in this method. The constraints should be selected very carefully or the result may be impractical.

Negrao and Simoes [38] considered a multi objective function formulation consists stress constraints on matearils used, concrete for pylons, and cost of materials.

Maximum/minimum stresses in stays, geometry control for box girder and deflections under dead load are set as constraints by Simoes and Negrao [38], [39] to optimize two cable-stayed bridges with box-girder decks.

Zero Displacement Method

The zero displacement method assumes that if the structure reaches the continuous beam deflection after construction, the ideal state of is reached and the initial cable forces are determined. The method is described by Wang et al. [40], [41]. The straight and horizontal bridge decks are considered in this method, in which the horizontal components of the cable forces will have no contribution on the bending moment. Hence, the bending moment distribution of the structure with zero displacements and the equivalent continuous beam will resemble each other.

Force Equilibrium Method

According to Chen et al. [42], the bending moment distribution at the initial stage is more important than the displacements whether zero or not as it affects the long term behaviour of the bridge by the redistribution of internal forces.

Since the method deal only with the force equilibrium, the nonlinearities arising from cable sag does not need to be involved in the process. Hence, the cable weights can be neglected. However, it is necessary take them into account to define the appropriate final geometry and decide for an appropriate precamber.

Cable anchor points are involved in the calculation as control parameters which are girder and tower anchor points. The bending moment distribution of the equivalent continuous beam is the target for this method with zero bending moments at tower section. [6], [7], [42].

Analysis Results

Effective modulus of elasticity approach is utilized for the consideration of the nonlinear cable sag effect. The stays are modelled by single truss elements.

The followings are considered for the analysis to find the initial tension forces.

a. Excessive changes in cable forces should be avoided.
b. Bending moment of steel girders should be reduced and made uniform
c. The main tower should have little displacement in longitudinal direction (bending moment of the main tower $M \to 0$).
d. There should be no void of cable tension
e. Cable section should be uniform

The bending moments of the girder and the pylons are depicted in Figure 5.7.

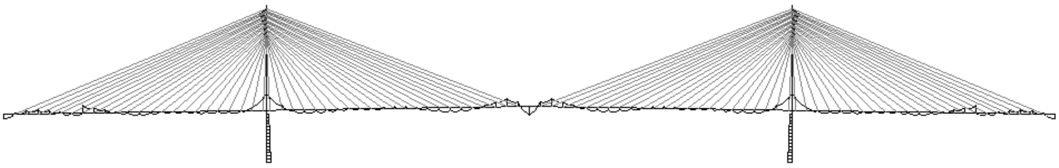

Figure 5.7 : Bending moment distribution in deck (dead load).

The bending moment distribution of the final state of the bridge deck and pylons and the equivalent continuous beam are in satisfactory accordance. The maximum moment of the pylons is 16.3 MNm which is very small.

The deformed shape, Figure 5.8, under the effect of dead load and superimposed dead load after applying the pretension forces on each cable. The maximum deflection at the deck is 0.1405 m in vertical direction which is compensated by the precamber. The maximum deflection of the pylons is 0.01 m in the longitudinal direction of the bridge which is converging to zero as intended.

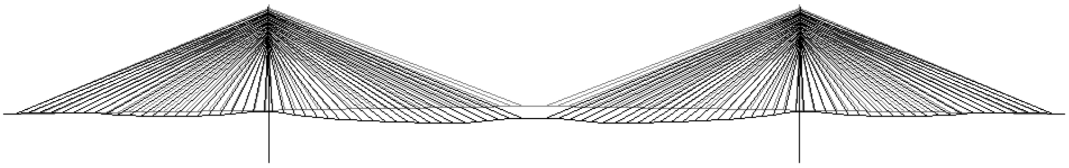

Figure 5.8: Dead load deformed shape (scaled).

Cables are grouped due to their installation order on the bridge. These are depicted in Figure 5.9.

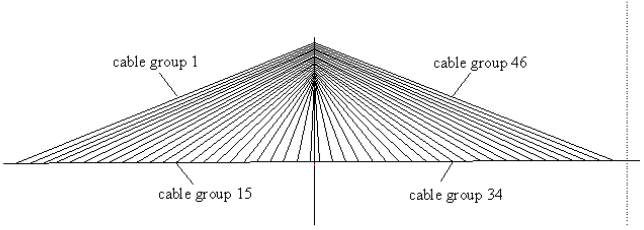

Figure 5.9 : Cable Groups.

5.3.2 Vehicular Live Load

There are six traffic lanes with 3600 mm width of each. Influence lines are obtained to determine the live load forces.

AASHTO design vehicular live load, HL93, is a combination of a “design truck” or “design tandem” and a “design lane”. A permit vehicle, P13 according to CALTRANS, loading is also considered.

Simultaneous lane occupation of the live load is taken into account by multipresence factors defined in AASHTO-LRFD [35] which are depicted in Table 5.9.

Application of the design vehicular live load is considered as in AASHTO-LRFD Article 3.6.1.3 [35].

The maximum effect is resulted from the loading that considers the negative moment between points of contraflexure under a uniform load on all spans and the reaction at interior piers only.

Table 5.9 : Multiple Presence Factors *m*

Number of Loaded Lanes	Multiple Presence Factors *m*
1	1.20
2	1.00
3	0.85
> 3	0.65

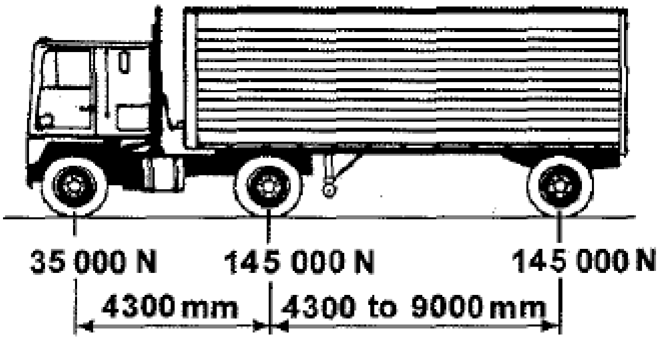

Figure 5.10 : AASHTO-LRFD design truck.

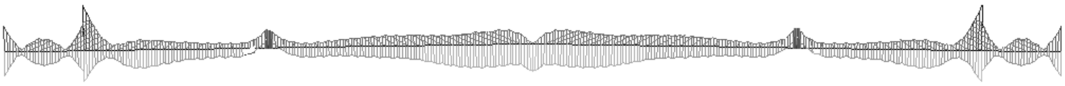

Figure 5.11 : Maximum and minimum bending moments in deck.

Maximum moment in the deck under live load conditions is 276.5 MNm at maximum and – 114.8 MNm which are depicted in Figure 5.11 for STRENGHT I combinations.

Deflection criteria is checked according to the SERVICE I combination. The maximum vertical deflection is 0.86 m. For most long-span cable-stayed bridges it is acceptable limits for the deflection between 1/400 and 1/500 of the central span length.

5.4 Earthquake Records

The effect of vertical component of ground motions on steel box girder of long span cable-stayed bridges is the main objective of this study. Vertical component of ground motions have been studied for two decades on the contrary of horizontal component which is extensively studied by many researchers.

First research concerning the effects of vertical component on bridges was conducted by Saadeghvaziri and Foutch [43]. They studied the inelastic behaviour of reinforced concrete columns using artificial horizontal and vertical ground motion records. The research showed that including vertical component in analysis resulted in considerably more damage when effective peak accelerations of 0.7 g than earthquake motions with effective peak acceleration equal to 0.4 g or less.

Some failure modes depending resulting from the vertical ground motion were reported by Broderick and Elnashai [44] and Papazoglou and Elnashai [45].

Yu [46] and Yu et al. [47] conducted a research on the effects of vertical component of ground motion on piers. Sylmar Hospital, Northridge record was used in analysis and the results reported as %21 increase in axial force and a %7 increase in the longitudinal moment on pier.

Button et al. [48], conducted a study with six different bridges covering variety of structural system parameters subjected to several ground motions. However, these studies were limited to linear response spectrum and linear time history analysis.

Veletzos et al. [49] investigated the effects of vertical component on precast segmental superstructures and they concluded the average positive bending rotations increase about 400% percent.

Recently Kunnath et al. [50], studied the effect of vertical component of several configurations of typical highway overcrossing. They carried out nonlinear response history analysis and concluded that the vertical component of ground motion cause significant amplification in the axial force demand in the columns and moment demands in the girder at both the midspan and at the face of the bent cap. Midspan moments in the girder found to exceed the capacity which lead to severe damage.

S waves which are the main cause of horizontal components are longer than P waves which cause propagation of the vertical component hence, vertical component has much higher frequency content. In result, vertical component lead to large amplifications in the short period range. [45], [51].

Unlike short-to-medium span bridges, there no code specified criteria to select ground motions for long-span bridges. To obtain accurate and meaningful response, selection of earthquake records for use of analysis is very important. Three criteria is utilized as described below.

PGA/PGV Ratio:

A selection criteria for the non-specific region applications suggested by Broderick and Elnashai [44]. The ratio peak ground acceleration to peak ground velocity, PGA/PGV (Zhu et.al) is employed for this study. Records will have high acceleration peaks of short duration which cause low velocity cycles when they measured on rock or resulted from near-source shallow earthquakes. This leads high values of PGA/PGV ratios. On the contrary, records will have lower acceleration values, but individual cycles are of longer duration which cause high velocity waves when they measured on soft ground or resulted from deep earthquakes, and this leads low values of PGA/PGV ratios. Hence, the records have high acceleration periods with longer duration periods tend to impose higher demand on long period structures [52]. The PGA/PGV ratio ranges are depicted in Table 5.10.

Table 5.10 : PGA/PGV Ratio Range (adapted from [52])

	Range
low	PGA/PGV < 0.8
medium	0.8 ≤ PGA/PGV ≤ 1.2
high	1.2 < PGA/PGV

V / H (Peak Ground Acceleration Ratio):

Many design codes using a 2/3 ratio of vertical component to horizontal component of ground motion, which was first suggested by Newmark [53]. Studies conducted by Abrahamson and Litehiser [54], Ambraseys and Simpson [55], Elgamal and He [56], Bozorgnia and Campbell [57], showed that V/H ratio of 2/3 is an underestimated value. In addition Elnashai and Papazoglou [45] stated that this value of V/H ratio is unconservative in the near-field while it is overconservative in the far-field.

Time interval between horizontal and vertical peak values:

Relationship between the timing of peak responses in the vertical and horizontal components of ground motion is also have a significant effect on response of structures in two ways. First, shakedown may be caused by earlier arrival of vertical component than the horizontal component of ground motion. Secondly, coincidence of these two components may cause significant amplification of the response of structural elements [51].

A study including 452 earthquake records was carried out by Kim et al. [51] to obtain the above mentioned V/H ratio and time interval characteristics with respect to distance to source and earthquakes. The results of this study are depicted in Figure 5.12.

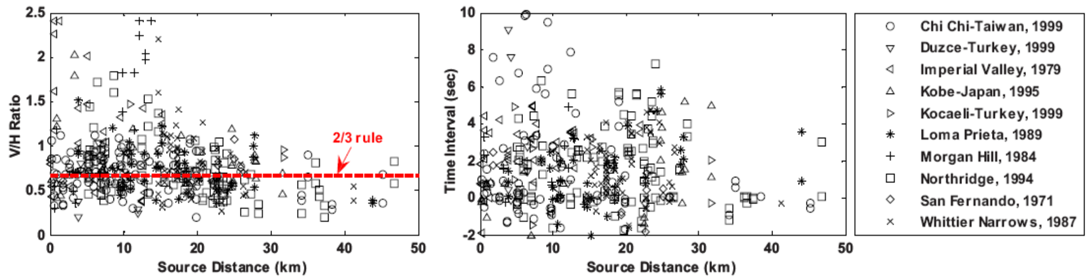

Figure 5.12 : (a) Distribution of V/H Ratio; **(b)** time interval [51].

In light of the above mentioned three criteria, two near-source earthquake records are selected from Pacific Earthquake Engineering Research Center Ground Motion Database. Ground motion records, depicted in Table 5.11, are selected to evaluate the performance of the long-span bridge. Fundamental periods of the bridge is given in Table 5.12.

Table 5.11 : Selected Ground Motions

Earthquake	Mw	Station	Distance (km) CD*	PGA (g) Long	PGA (g) Trans	PGA (g) Vert	PGV (m/s)	PGA/ PGV	V/H
Imperial Valley (1979)	7.62	Array #6	0.3	0.439	0.410	1.660	1.098	0.40	3.78
Kocaeli (1999)	7	Yarimca	4.8	0.349	0.268	0.242	0.690	0.51	0.69
Chi Chi (1999)	6.53	TCU068	1.4	0.566	0.462	0.486	1.873	0.30	0.86

* CD=closest distance to fault

Table 5.12 : Fundamental Periods of IY 700

Fundamental Periods Vertical (sec)	Fundamental Periods Longitudinal (sec)	Fundamental Periods Transverse (sec)
5.04	3.97	6.55

Both fast Fourier transform (FFT) and response spectral analysis are studied to define the predominant frequency of the selected ground motions with SeismoSignal [58]. 2% damping is utilized for the response spectral analysis. Figures from 5.13 to 5.21 and Table 5.12 show the period characteristics and frequency contents of the selected records.

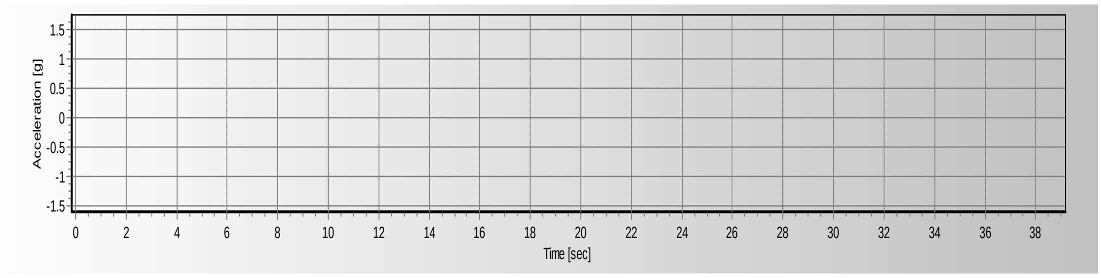

Figure 5.13 : Time – acceleration of Imperial Valley vertical component.

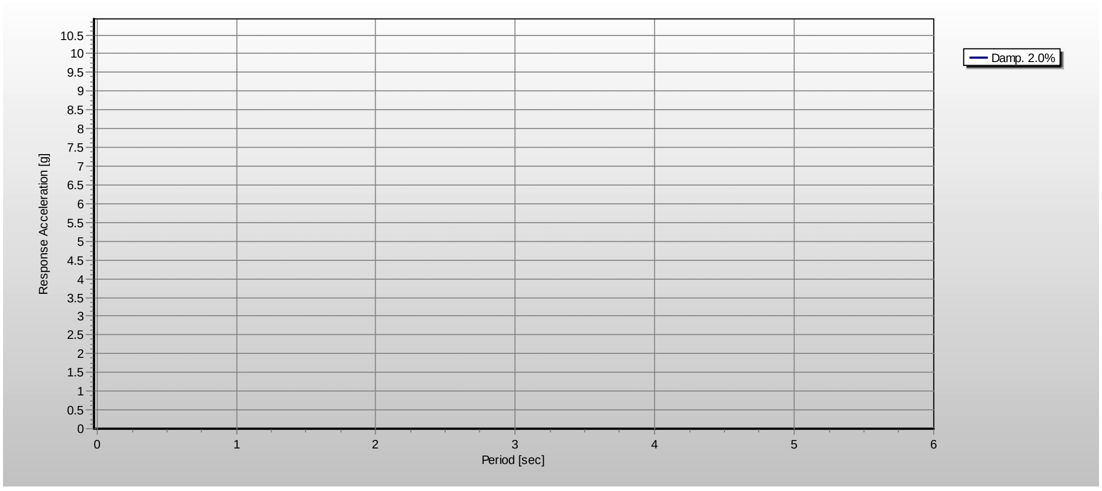

Figure 5.14 : El Centro Array #6 – Vertical Component Response Spectrum.

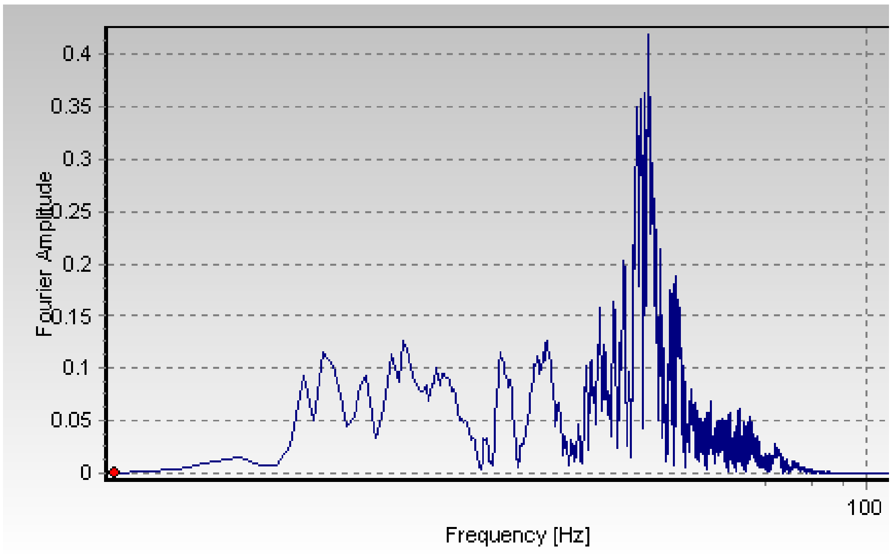

Figure 5.15 : El Centro Array #6 – Vertical Component FFT.

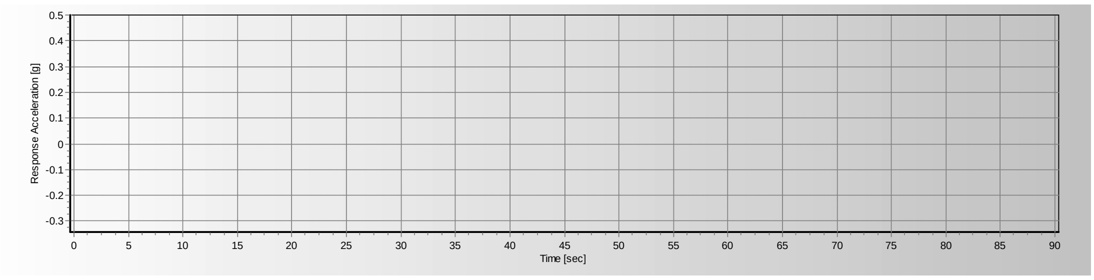

Figure 5.16 : Time – acceleration of Chi Chi vertical component.

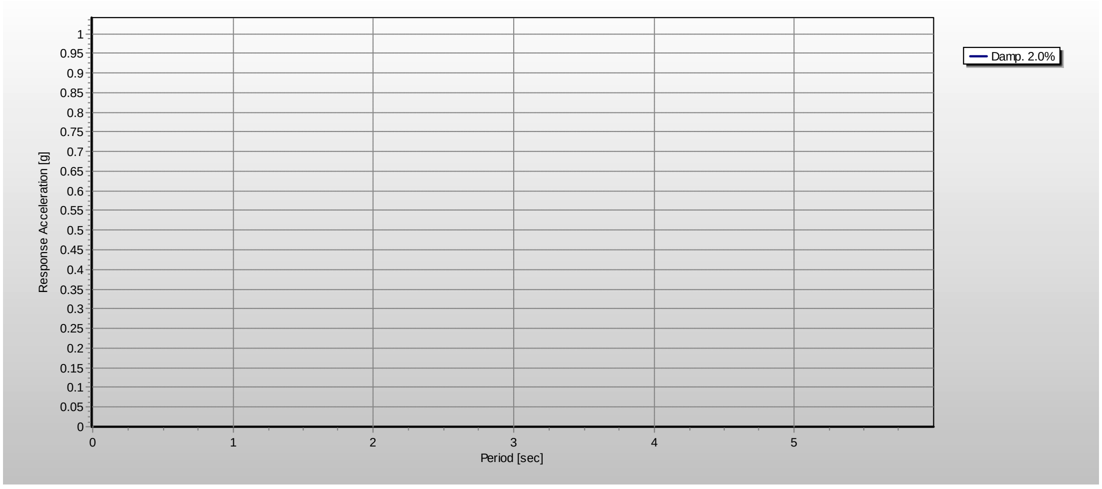

Figure 5.17 : Chi Chi Taiwan, TCU068 – Vertical Component Response Spectrum.

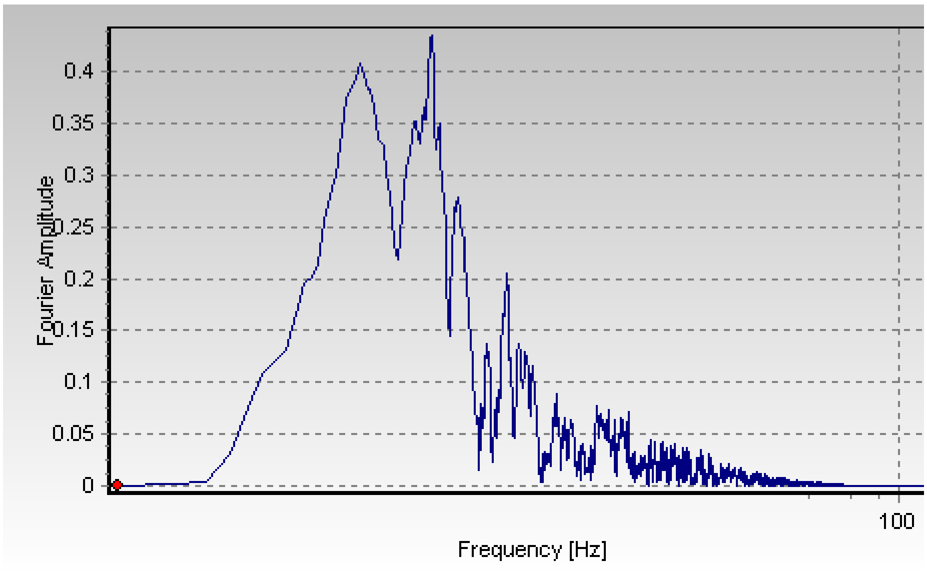

Figure 5.18 : Chi Chi Taiwan, TCU068 – Vertical Component FFT.

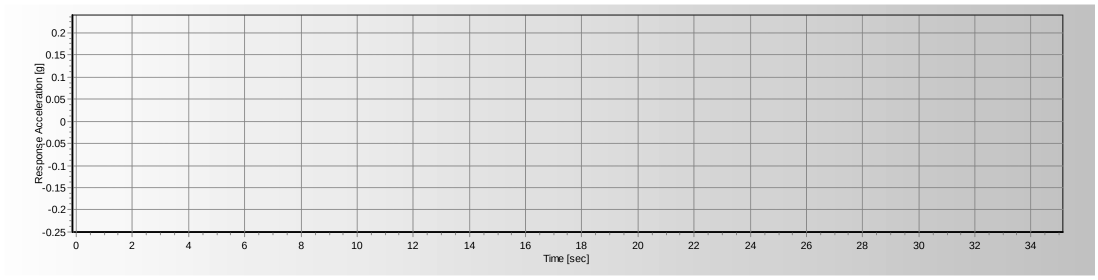

Figure 5.19 : Time – acceleration of Kocaeli vertical component.

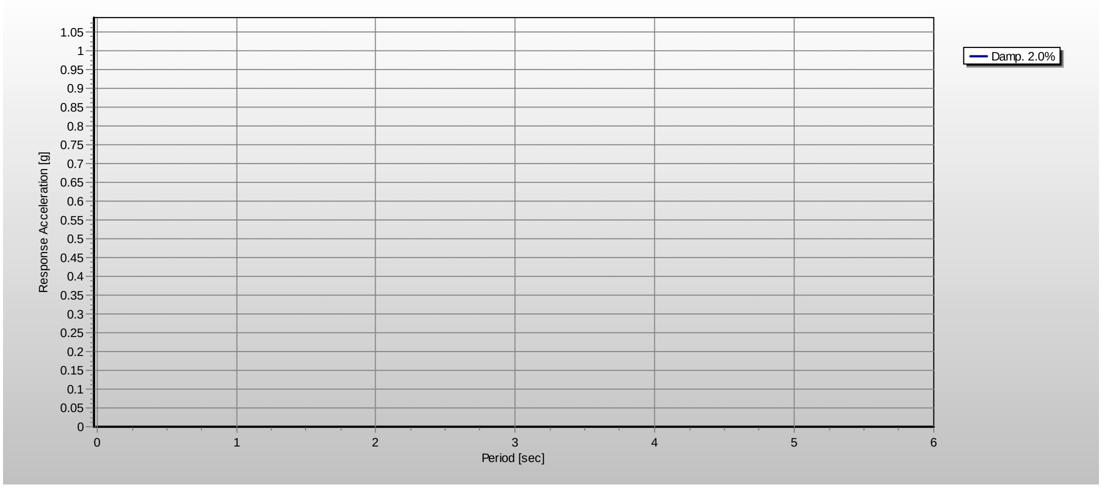

Figure 5.20 : Kocaeli, Yarimca – Vertical Component Response Spectrum.

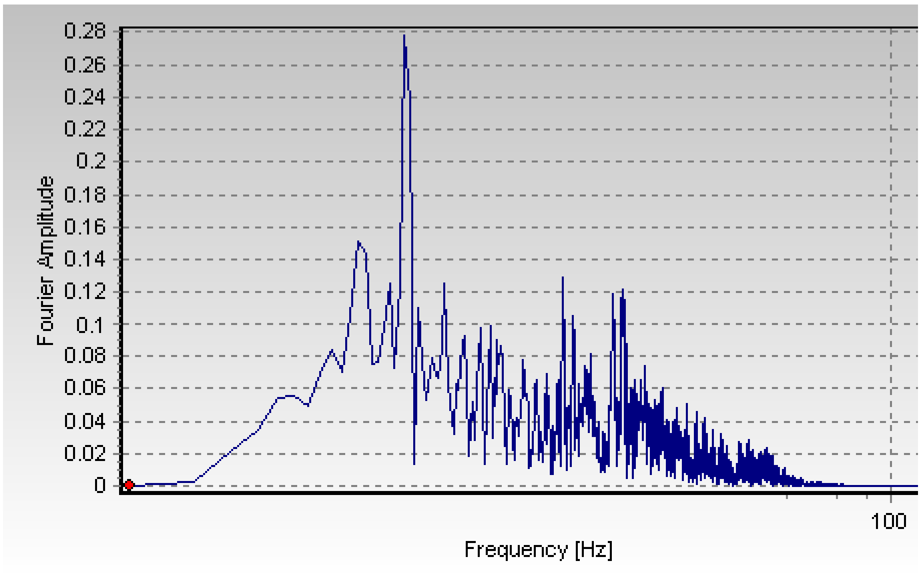

Figure 5.21 : Kocaeli, Yarimca – Vertical Component FFT.

The rationale behind the selection of the above given ground motions can be stated as;

1 - El Centro Array #6 is the most commonly used earthquake record for the studies of long-span cable-stayed bridges by many researchers.

2 - The Chi Chi ground motion is a not only near-fault but also pulse-type ground motion. Pulse-type ground motions are not considered in any seismic codes except UBC 1997.

3 - Kocaeli, Yarimca record is representing the mediocre ground motion event on the basis of comparison of these selected ground motions.

5.5 Damping Characteristics

A structural damping of %2 is applied as Rayleigh damping and used for all analysis. Damping characteristics of cable-stayed bridges were explained in extend in Section 2. Besides that, later Elnashai and Papazoglou [45] and Collier and Elnashai [59] explained that the vertical component of ground motion is associated with higher frequencies, hence suggested to limit the damping ratio of %2.

Rayleigh coefficients are computed depending on a deck mode and a tower mode with high mass participation.

6.CHARACTERISTICS OF THE BRIDGE

6.1 Static Characteristics of the Bridge

Cable supported long span bridges are distinguished from most of the structures because of their long spans and flexibility.

The bridge which is considered in this study found to satisfy all strength and service limit states that considered among the relative displacements.

6.2 Dynamic Characteristics of the Bridge

The eigen value analysis is performed to obtain dynamic behaviour characteristics with utilization of the tangent stiffness matrix of the dead load deformed state [4], [24]. Boundary conditions considered for the modal analysis are given in Table 6.1.

Table 6.1 : Boundary Conditions

	x - direction (longitudinal)	y - direction (transverse)
Deck - Pylon	free	fixed
Intermediate Piers	fixed	fixed
End Piers	fixed	fixed

First fifteen modes, their nature, periods, frequencies and mass participation ratios are depicted in Table 6.2. First modes are all deck modes and first two mode shapes are depicted in Figures 6.1 and 6.2.

The fundamental mode with period 6.55 s is a torsional lateral mode as depicted in Figure 6.1.

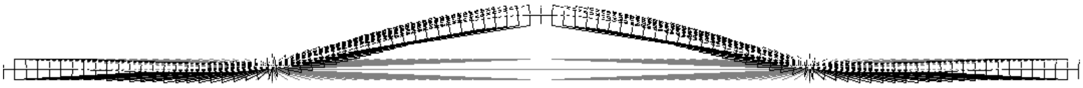

Figure 6.1 : Fundamental Mode, TL 1

Table 6.2 : First 15 modes

Mode No	f [cyc/sec.]	T [sec.]	Modal mass x [%]	Modal mass y [%]	Modal mass z [%]	Nature	Dir.
1	0.15	6.55	0.00	20.20	0.00	TL 1	y
2	0.20	5.04	0.00	0.00	7.19	V 1	z
3	0.25	3.97	4.39	0.00	0.00	V 2	x
4	0.34	2.95	0.00	0.00	0.00	TL 2	y
5	0.35	2.90	0.00	1.80	0.00	TL 3	y
6	0.35	2.87	0.00	1.12	0.00	TL 4	y
7	0.36	2.78	0.00	0.00	0.00	TL 5	y
8	0.37	2.72	0.00	0.00	0.22	V 3	z
9	0.39	2.59	0.00	48.40	0.00	TL 6	y
10	0.43	2.34	19.96	0.00	0.00	V 4	x
11	0.48	2.07	0.00	0.00	0.00	TL 7	x
12	0.50	2.01	0.00	0.00	3.94	V 5	z
13	0.56	1.77	0.00	0.00	0.00	TL 8	y
14	0.58	1.73	6.75	0.00	0.00	V 6	x
15	0.62	1.62	6.41	0.00	3.63	TL 9	x

*TL identifies torsional lateral modes, V identifies vertical modes

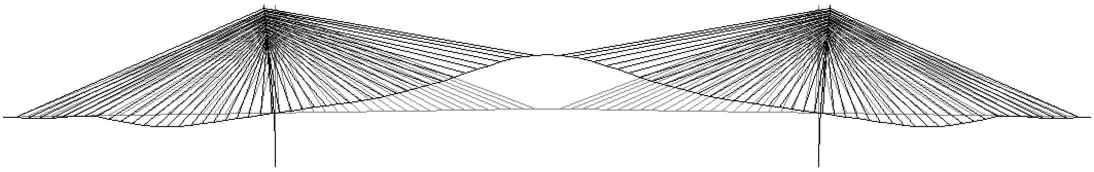

Figure 6.2 : 2nd Mode, V 1.

Period distribution of the structure is depicted in Figure 6.4. First 11 modes have periods above 2s and periods below 2s are closely spaced.

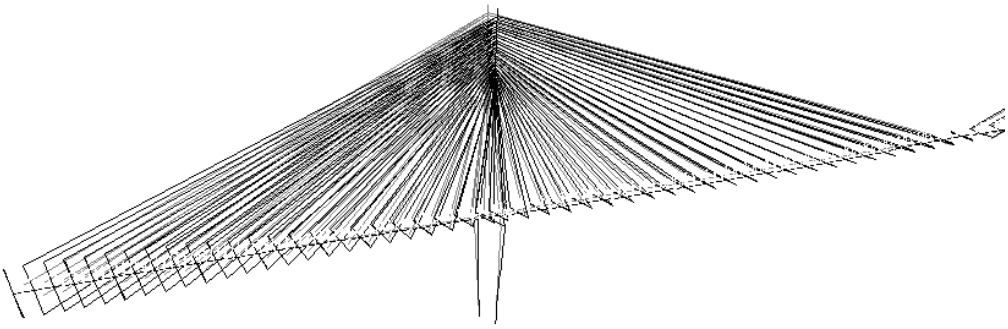

Figure 6.3 : 4th Mode, TL 2.

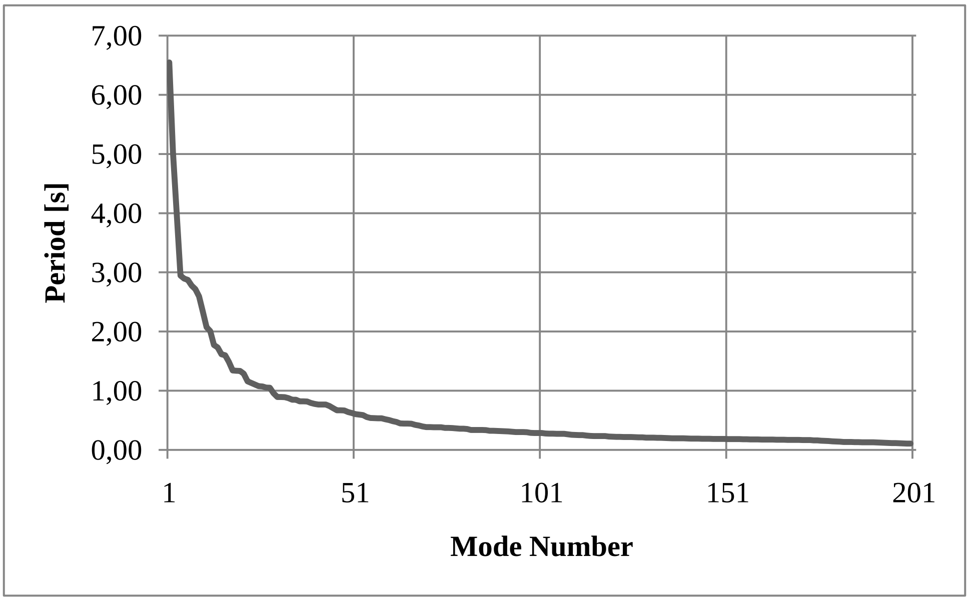

Figure 6.4 : Period distribution.

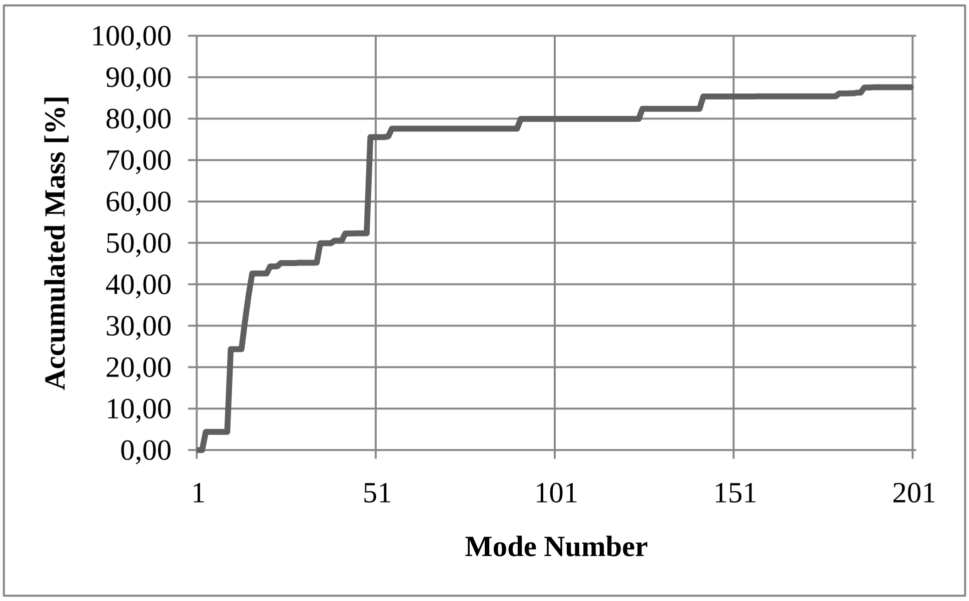

Figure 6.5 : Modal mass participation in longitudinal direction.

If model support conditions are selected as free in transverse (lateral) direction, then the fundamental period of the bridge will result in the period of a pendulum which is formulated by Galileo Galilei and the nature of this mode will be transverse sway.

$$T_{pendulum} = 2\pi\sqrt{\frac{l}{g}} \qquad \textbf{(6.1)}$$

Where,

l : the distance between pylon top and deck

g : acceleration of gravity

$$T_{pendulum} = 2\pi\sqrt{\frac{139m}{g}} = 23.651 \text{ sec.}$$

Since the period is calculated as 22.394 sec. by modal analysis, the deck is a bit stiffer than the equivalent system.

7. EARTHQUAKE RESPONSE

7.1 Introduction

Nonlinear time history analysis is carried out, after a nonlinear static load analysis under dead load, to obtain seismic response characteristics of the bridge.

Bending moment change at midspan, at the face of crossbeam of the pylon, and intermediate pier are investigated among the rotation displacements.

7.2 Nonlinear Time History Analysis

Nonlinear direct integration method is adopted for dynamic analysis of the bridge.

- Newmark implicit integration sheme ($\delta = 0.5$, $\alpha = 0.25$)
- Time step, $\Delta t = 0.02$ which allows high frequency modes to participate in response. A sensitivity analysis should be carried out usually, however the value suggested by many researchers is used in this study.
- Geometric nonlinearity is considered

7.3 Results

The results obtained by nonlinear time history analysis will be given in this section. My refers to the longitudinal bending moment and Ry refers to rotational deformations on the girder. Figure 7.1 showing elements and nodes in consideration.

H+L is representing values resulting from only horizontal ground motion excitation, H+L+V is representing values obtained by including the vertical component of ground motion to horizontal components in the following figures.

A parametric study is carried out depending upon PGA/PGV ratios and V/H ratios. Response of bridge which is subjected to only horizontal components and both horizontal and vertical components are given below in detail.

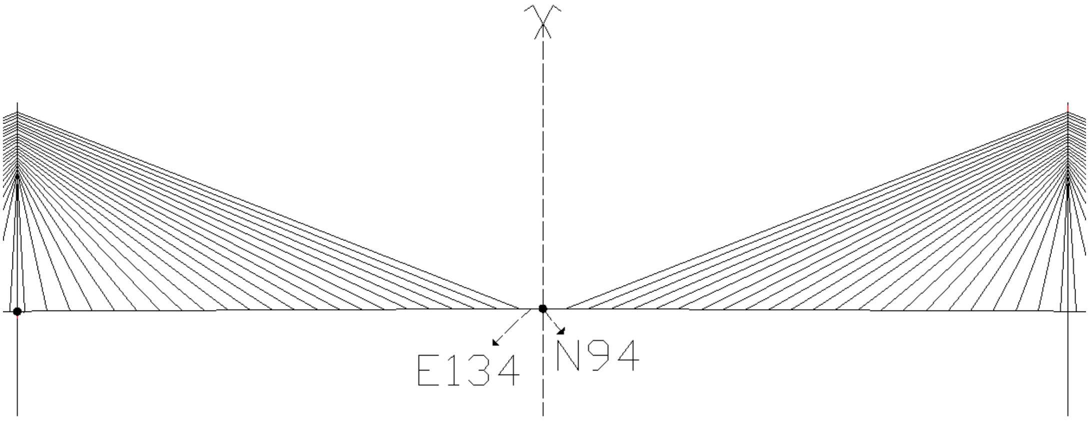

Figure 7.1 : Element and node of girder considered at midspan for response.

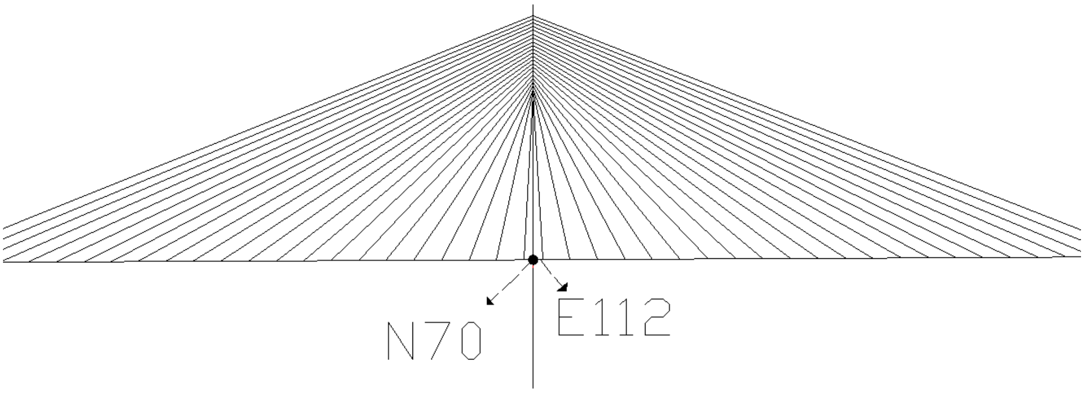

Figure 7.2 : Element and node considered at pylon section of girder for response.

Kocaeli, Yarimca:

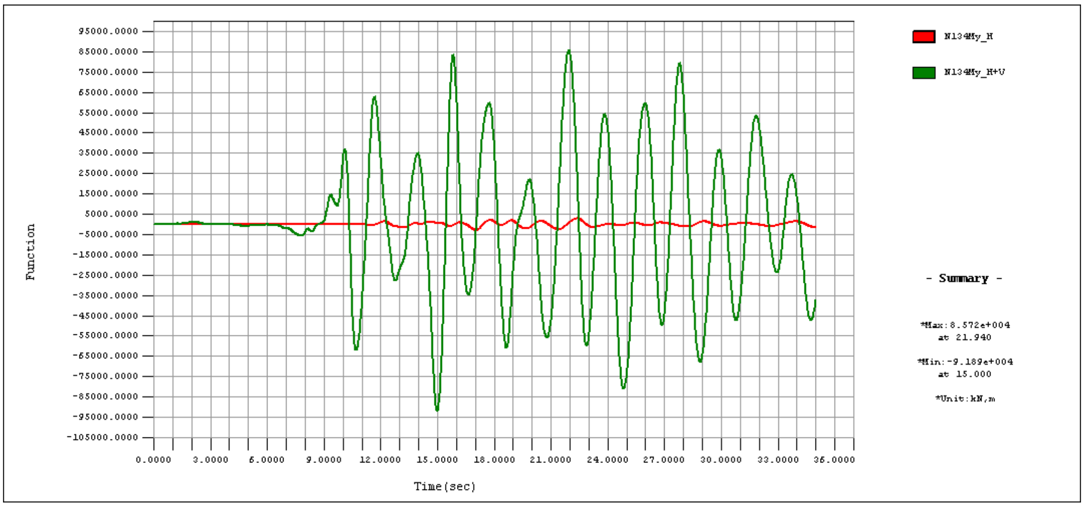

Figure 7.3 : E134 – My Moment.

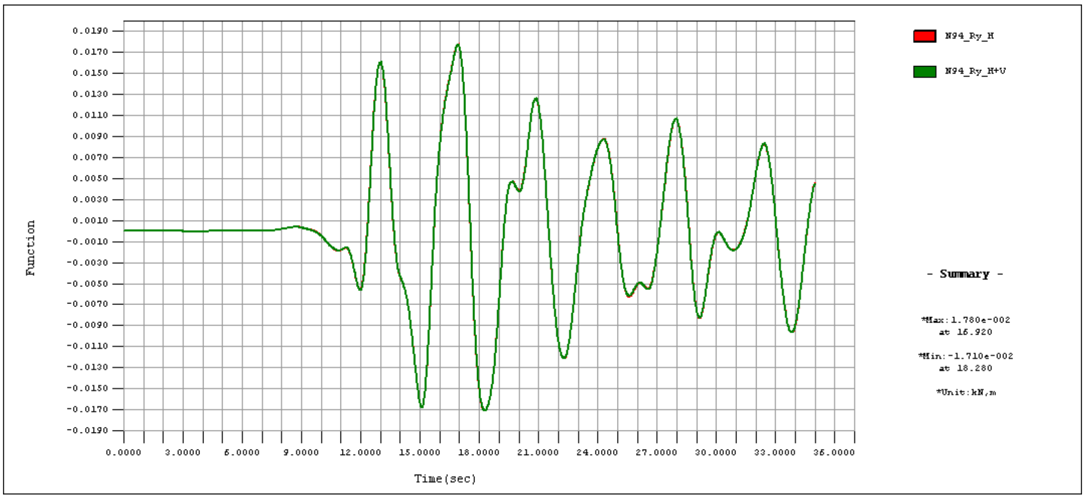

Figure 7.4 : N94 – Ry Displacement.

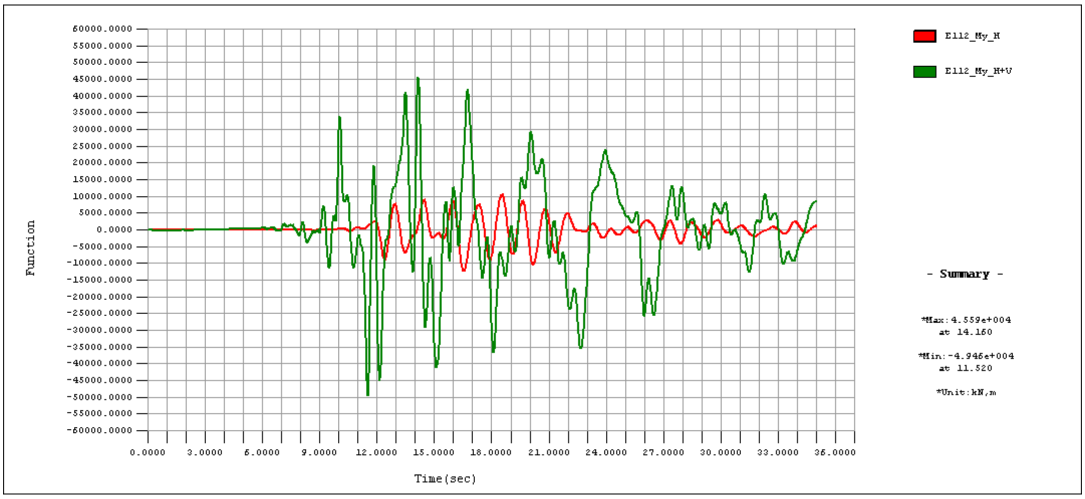

Figure 7.5 : E112 – My Moment.

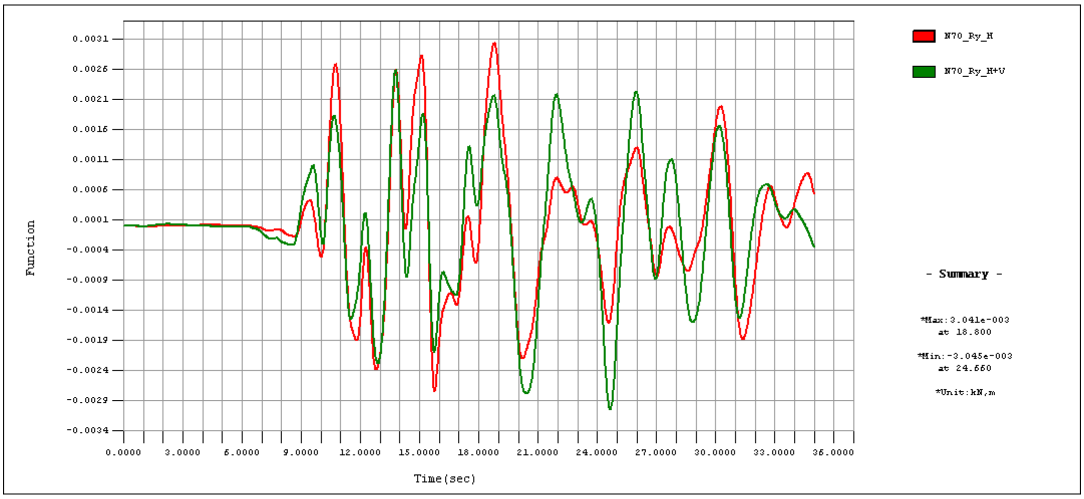

Figure 7.6 : N70 – Ry Displacement.

Moments resulting from the excitation of ground motion including vertical component are seriously amplified when they compared with moments resulted from only horizontal ground motion excitation at the midspan, Element 134. It is depicted in Figure 7.3.

On the contrary, rotations about y axis of the bridge do not change due to participation of the vertical component of earthquake at the midspan, Node 94. As can be seen from Figure 7.4 change of rotation deformations in time resulting from both cases are exactly same.

At the pylon section of stiffening girder, Element 112, moments resulting from the excitation of ground motion including vertical component are also found to be increased they compared with moments resulted from only horizontal ground motion. The rate of amplification is depicted in Figure 7.5.

In addition, rotations about y axis of the girder are amplified by the contribution of vertical component of earthquake.

ElCentro, Array # 6:

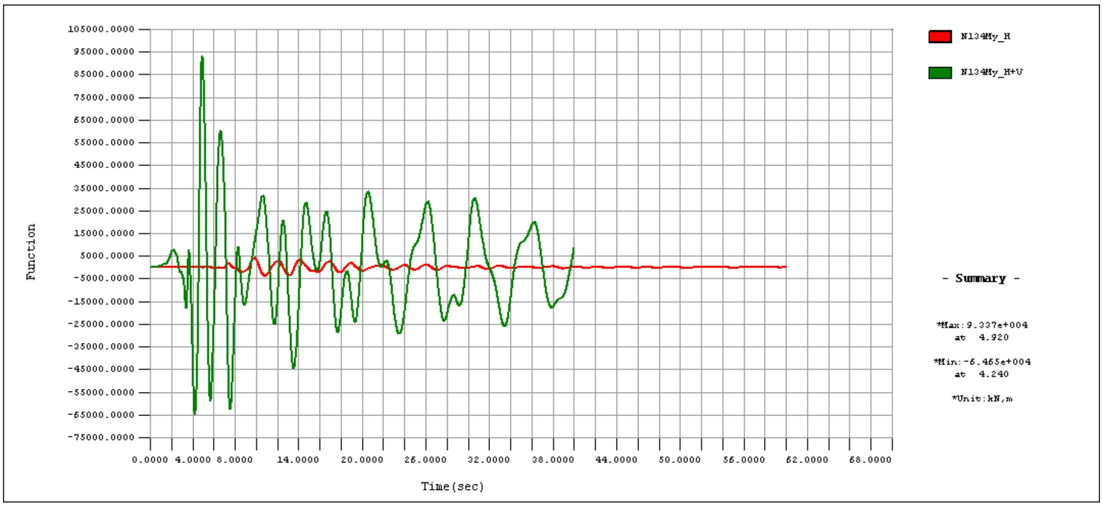

Figure 7.7 : E134 – My Moment.

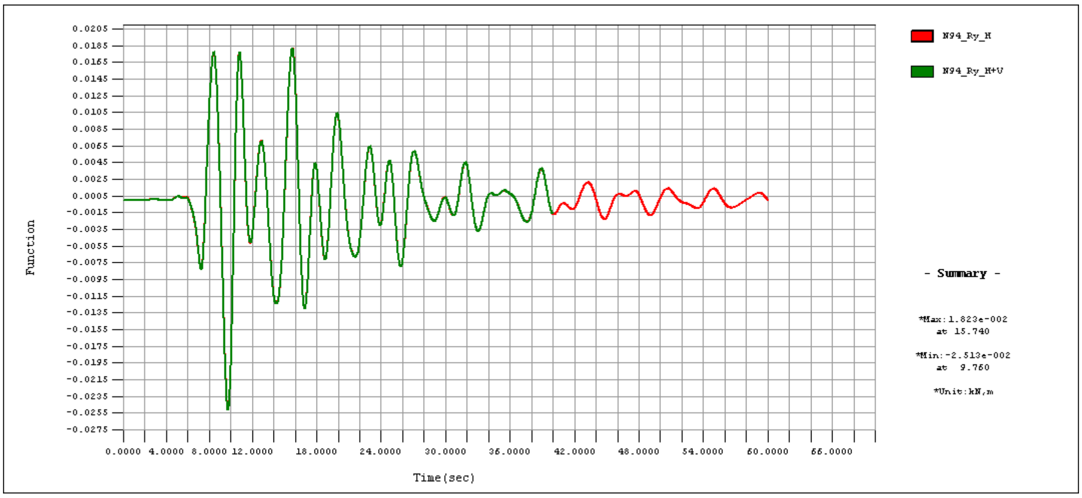

Figure 7.8 : N94 – Ry Displacement.

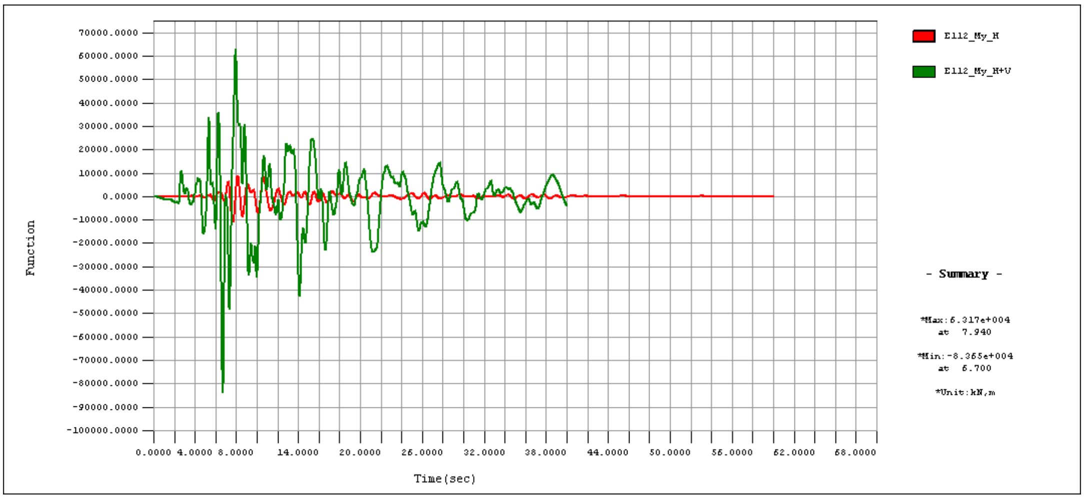

Figure 7.9 : E112 – My Moment.

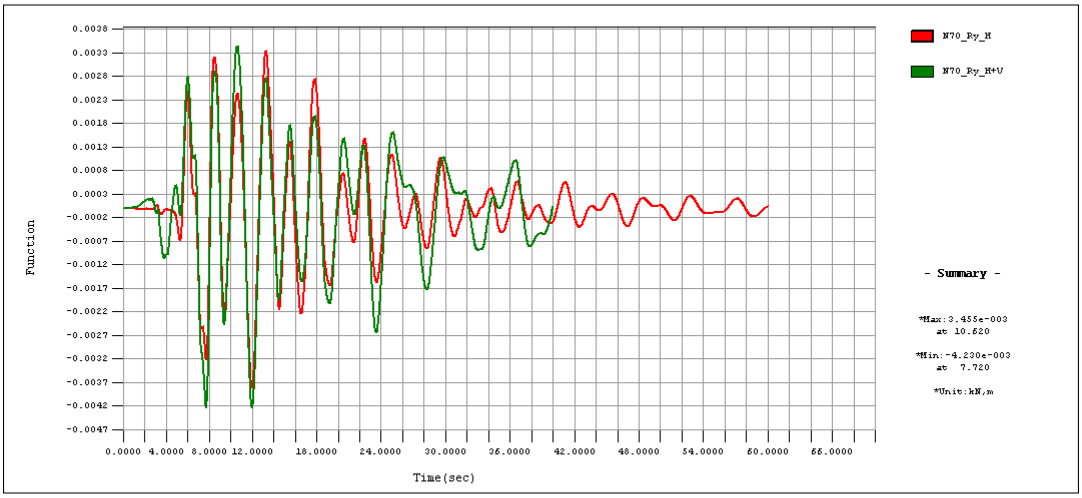

Figure 7.10 : N70 – Ry Displacement.

Chi Chi, TCU068:

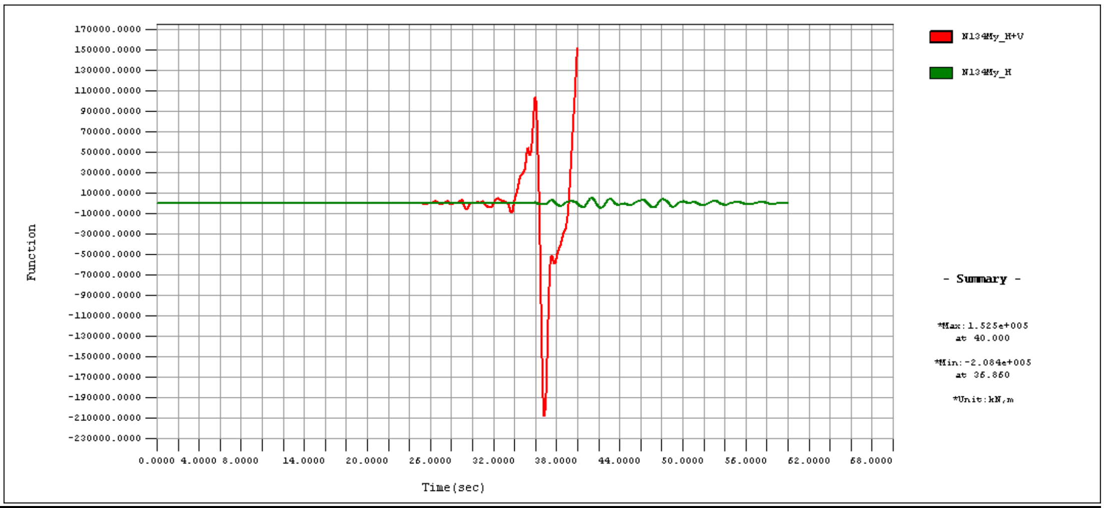

Figure 7.11 : E134 – My Moment.

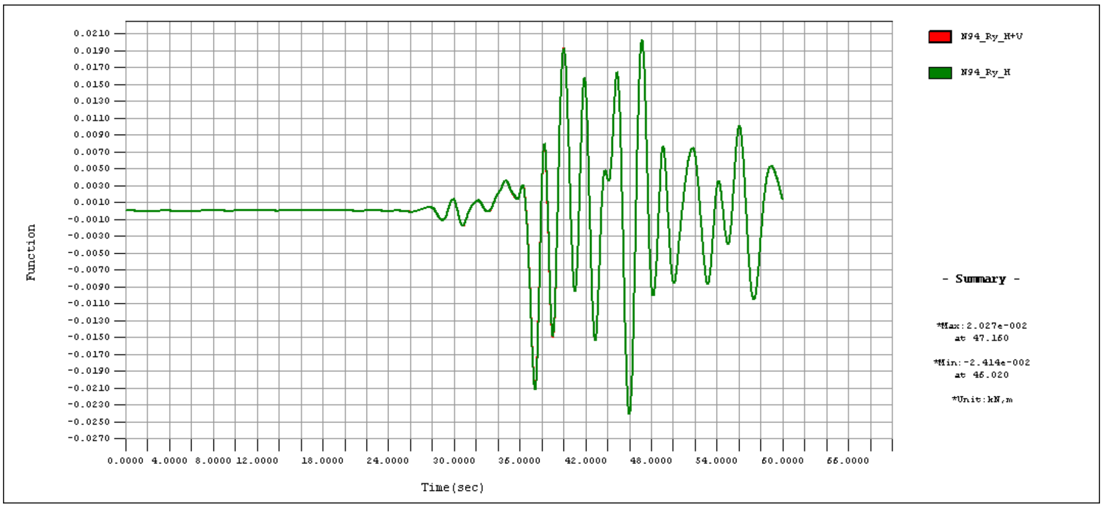

Figure 7.12 : N94 – Ry Displacement.

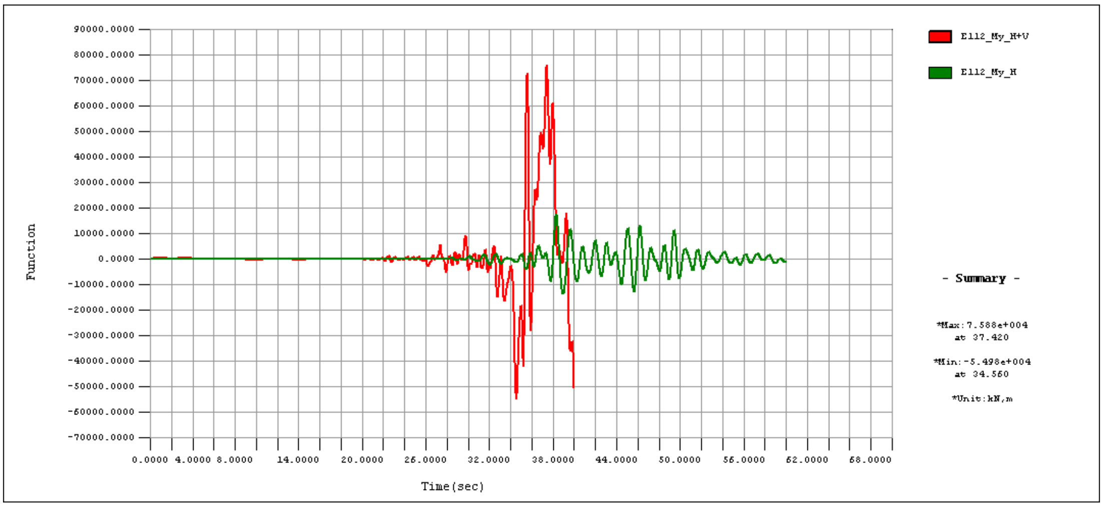

Figure 7.13 : E112 – My Moment.

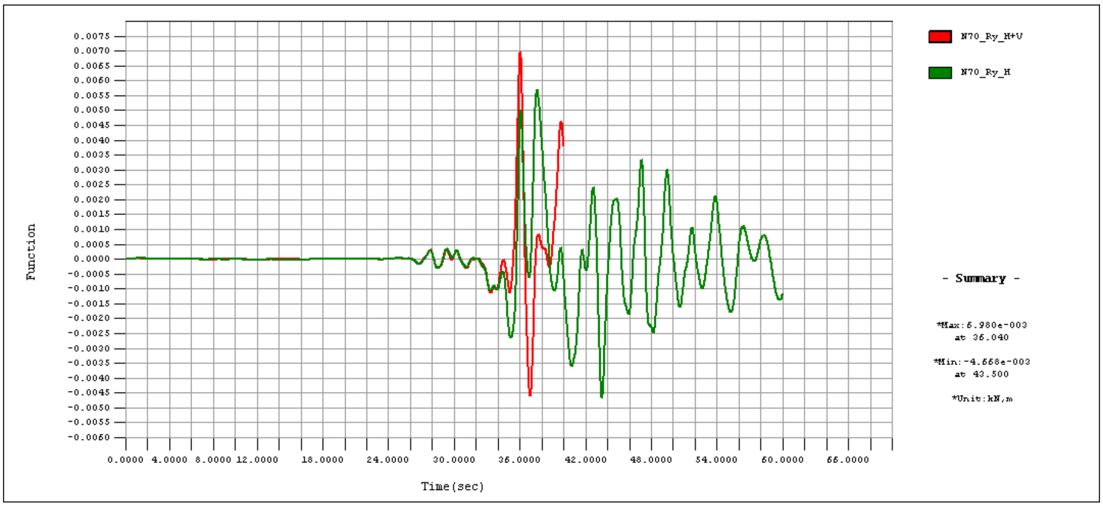

Figure 7.14 : N70 – Ry Displacement .

Experience show that, seismic load seldom controls the design except in extremely high seismic areas.

All results presented in Table 7.1 and Table 7.2 compare the code specified load combinations for design and the internal forces obtained from the contribution of the vertical component of the ground motions. The results in Table 7.1 and 7.2 are also include the normalized values by the corresponding response of the live load and dead load combination.

Table 7.1 : Comparison of moment values for element 134 between code specified load combinations

	Load	Elem. No.	$M_{max.}$	$M_{min.}$
	DL	134 (N94)	22677	
	DL + 1.75LL		**137964**	-2333
Kocaeli	DL + (TH- H)	134 (N94)	27746	-2836
	DL + (TH- HV)		85723	**-91890**
Imperial Valley	DL + (TH- H)	134 (N94)	27746	-3781
	DL + (TH- HV)		93368	**-64653**
Chi Chi	DL + (TH- H)	134 (N94)	27746	-4562
	DL + (TH- HV)		**152500**	**-208404**

Table 7.2 : Comparison of moment values for element 112 between code specified load combinations

	Load	Elem. No.	$M_{max.}$	$M_{min.}$	$M_{max.}$/DL	$M_{min.}$/LL
	DL	112 (N70)	22677		1,00	
	DL + 1.75LL		-35079	-106726	-1,55	1,00
Kocaeli	DL + (TH- H)	112 (N70)	10575	-49382	0,47	0,46
	DL + (TH- HV)		**46887**	-49382	2,07	0,46
Imperial Valley	DL + (TH- H)	112 (N70)	8948	-49382	0,39	0,46
	DL + (TH- HV)		**92663**	-49382	4,09	0,46
Chi Chi	DL + (TH- H)	112 (N70)	17703	-49382	0,78	0,46
	DL + (TH- HV)		**68960**	-90492	3,04	0,85

Table 7.3 : Increment ratio for rotational displacement of node 70.

	N70	time (s.)
Kocaeli	71%	23
Imperial Valley	143%	31
Chi Chi	522%	40

8. CONCLUSIONS

Vertical component of ground motions and its effects on structures has not been investigated in depth as much as the horizontal components. More research is needed on the subject of vertical component of ground motions, especially for the near fault strong motions.

Negative moment demand at the centre of the main span is considerably increased as depicted in Table 7.1. No variation observed at the deck negative moment demand at the face of pylon. Positive moment demand is increased as depicted in Table 7.2.

Rotational displacement demand of the deck at the face of the pylons is increased with 71% ratio at least as depicted in Table 7.3. This may be further studied in manner of ductility capacity of the deck.

These conclusions are in parallel manner with the conclusions derived by Kunnath et al. [50] for short span crossover bridges. Also, it has been concluded that vertical component effects may be uncoupled from the horizontal component effects as depicted in Figures 7.3, 7.5, 7.7, 7.9, 7.11, 7.12.

In addition to above stated, it has been concluded that the impulse character of the vertical component of ground motion, as in Chi Chi, Taiwan record, impose the most demand on midspan deck negative moment and rotational displacement capacity of the deck at the face of the pylon.

Selection of the ground motions by means of predominant frequency of the ground motion is also an important criteria for obtaining effects of the vertical component.

Due to these results, the effect of the vertical component of the selected ground motion should carefully examined, especially for the near fault ground motions.

Isolation devices may be used to reduce the response of cable-stayed bridges. In addition support conditions may be revised to provide more flexible structure as concluded by many researchers before.

It is obvious that due to exceptional and unique nature of each long span cable-stayed project, a code specification is not possible. However, since the behaviour of the structure in earthquake prone areas has been the major source of concern, guidance for selection of ground motions is necessary for use of design firms.

As investigated by many researchers before, the effect of the vertical component of the ground motion can cause severe amplification in the bridge response. Hence, it should be included in dynamic analysis of long span bridges with appropriate earthquake records selected to result in accurate and meaningful response characteristics.

REFERENCES

[1] **Nazmy, A. S., Abdel-Ghaffar, A. M.,** 1987 : Seismic Response Analysis of Cable-Stayed Bridges Subjected to Uniform and Multi-Support Excitations. *Report No. 87-SM-1*, Department of Civil Engineering, Princeton University, Princeton, N.J.

[2] **Cho, S., et al.,** 2009 : Incheon Bridge: Facts and the State of the Art, *International Commemorative Symposium for the Incheon Bridge*, Korea, pp. 18 – 29.

[3] **Son, Y., et al.,** 2009 : Design & Construction of Incheon Bridge CSB Pylon, *International Commemorative Symposium for the Incheon Bridge*, Korea, pp. 120 – 133.

[4] **Masashi, Y., et al.,** 2003 : Design of “Tatara Bridge”, *IHI Engineering Review*, Vol. **36**, No. **2**, pp. 40 – 56.

[5] **Chen, W. F., Duan, L.,** 2000 : Bridge Engineering Handbook. *CRC Press LCC.*

[6] **Troitsky, M. S.,** 1988 : Cable-Stayed Bridges: Theory and Design. 2nd Edition.

[7] **Gimsing, N. J.,** 1998 : Cable Supported Bridges – Concept & Desgin. *John Wiley*, 2nd Edition.

[8] **Walther, R. et al.** 1999 : Cable Stayed Bridges. *Thomas Telford*, 2nd Edition.

[9] **Tang, M. C.,** 1983 : Concrete cable-stayed bridges, presented at ACI Convention, Kansas City.

[10] **Tang, M. C.,** 1971 : Analysis of cable-stayed bridges, *Journal of the Structural Division ASCE.*

[11] **Podolny, N. J., Scalzi J. B.,** 1986 : Construction and Design of Cable-Stayed Bridges. *John Wiley & Sons*, 2nd Edition.

[12] **Ren, W. X., Obata, M.,** 1999 : Elastic-Plastic Seismic Response of Long Span Cable-Stayed Bridges, *Journal of Bridge Engineering*, Vol. **4**, pp. 194-203.

[13] **Fleming, J. F., Egeseli, E. A.,** 1980 : Dynamic Behaviour of a Cable-Stayed Bridge. *Earthquake Engineering and Structural Dynamics*, Vol. **8**, pp. 1 – 16.

[14] **Nazmy, A. S., Abdel-Ghaffar, A. M.,** 1990 : Non-linear earthquake response analysis of long-span cable-stayed bridges: theory, *Earthquake Engineering and Structural Dynamics*, Vol. **19**, pp. 45 – 62.

[15] **Nazmy, A. S., Abdel-Ghaffar, A. M.,** 1990 : Non-linear earthquake response analysis of long-span cable-stayed bridges: applications, *Earthquake Engineering and Structural Dynamics*, Vol. **19**, pp. 63 – 76.

[16] **Ernst, HJ.,** 1965 : Der E-Modul von Seilen unter Berücksichtingung des Durchhangens. *Bauingenieur*, Vol. **40**, pp. 52 – 55.

[17] **Abdel-Ghaffar, A. M., Khalifa, M.,** 1991: Importance of Cable Vibration in Dynamics of Cable-Stayed Bridges. *Journal of Engineering Mechanics*, Vol. **117**, pp. 2571 – 2589.

[18] **Abdel-Ghaffar, A. M., A. S. Nazmy,** 1991 : 3-D Nonlinear Seismic Behavior of Cable-Stayed Bridges. *Journal of Structural Engineering*, Vol. **117**, pp. 3456 – 3476.

[19] **Abdel-Ghaffar, A. M., A. S. Nazmy,** 1988 : Nonlinear Seismic Response of Cable-Stayed Bridges Subjected to Nonsynchronous Motion. *Proceedings of 9th World Conference on earthquake Engineering*, Tokyo-Kyoto, Vol. **6**, pp. 483 – 488.

[20] **Zienkiewicz, O. C., Taylor, R. L.,** 1991 : The Finite Element Method. *Mc Graw Hill* , 4th Edition, Vol. 1,2.

[21] **Abdel-Ghaffar, A. M., A. S. Nazmy,** 1986 : Seismic Behavior of Long-Span Cable-Stayed Bridges. *Dynamic Response of Structures*, American Society of Civil Engineers, New York, pp. 281-288.

[22] **Ali, H. M., Abdel-Ghaffar, A. M.,** 1995 : Modelling the nonlinear seismic behavior of cable-stayed bridges with passive control bearings. *Computers & Structures*, Vol. **54**, No. 3, pp. 461-492.

[23] **Wilson, J. C., Liu, T.,** 1991: Ambient Vibration Measurements on a Cable-Stayed Bridge. *Earthquake Engineering and Structural Dynamics,* Vol. **20**, pp. 723 – 747.

[24] **Kawashima, K.,** 2011 : Seismic Design of Urban Infrastructure. *Lecture Notes*, Tokyo Institute of Technology.

[25] **Daniell, W. E., MacDonald, J. H. G.,** 2007: Improved Finite Element Modelling of a Cable-Stayed Bridge Through Systematic Manual Tuning. *Engineering Structures*, Vol. **29**, pp. 358 – 371.

[26] **Nazmy, A. S., Abdel-Ghaffar, A. M.,** 1992 : Effeccts of Ground Motion Spatial Variabilty on the Response of Cable-Stayed Bridges. *Earthquake Engineering and Structural Dynamics*, Vol. **21**, pp. 1 – 20.

[27] **Kawashima, K., Unjoh, S., Tunomoto, M.,** 1993 : Estimation of Damping Ratio of Cable-Stayed Bridges for Seismic Design. *Journal of Structural Engineering*, Vol. **119**, pp. 1015 – 1031.

[28] **Clough, R. W., Penzien, J.** 1993 : Dynamics of Structures. *McGraw-Hill*, 2nd Edition.

[29] **Ali, H. M., Abdel-Ghaffar, A. M.,** 1995 : Modelling of Rubber and Lead Passive-Control Bearings for Seismic Analysis. *Journal of Structural Engineering*, Vol. **121**, pp. 1134-1144.

[30] **Ali, H. M., Abdel-Ghaffar, A. M.,** 1994 : Seismic Energy Dissipation for Cable-Stayed Bridges Unsing Passive Devices. *Earthquake Engineering and Structural Dynamics*, Vol. **23**, pp. 877 – 893.

[31] **Kawashima, K., Unjoh, S.,** 1992 : Damping Characteristics of Cable-Stayed Bridges, *Proceedings of the 10th World Conference on Earthquake Engineering*, Madrid, pp. 4803 – 4808.

[32] **Kawashima, K., Unjoh, S., Azuta, Y.-I.,** 1988 : Damping Characteristics of Cable-Stayed Bridges, *Proceedings of the 9th World Conference on Earthquake Engineering*, Tokyo-Kyoto, Vol. **6**, pp. 471 – 476.

[33] **Kawashima, K., Unjoh, S., Azuta, Y.-I.,** 1990 : Analysis of Damping Characteristics of a Cable-Stayed Bridge Based on Strong Motion Records, *Structural Engineering/Earthquake Engineering, Japan Society of Civil Engineers*, Vol. **6,** No. **1**, pp. 181 – 190.

[34] **Wilson, J. C., Liu, T., Gravelle, W.,** 1991: Ambient Vibration and Seismic Response of a Cable-Stayed Bridge. *European Earthquake Engineering*, Vol. **5**, pp. 9 – 15.

[35] **AASHTO**, LRFD Bridge Design Specifications, American Association of State Highway and Transportation Officials, Washington, D. C., 2010.

[36] **COSMOS/M,** 2008: User’s Manual, Solidworks Corporation, Dassault Systémes, Massachusetts, USA.

[37] **Wilson, J. C., Gravelle, W.,** 1991: Modelling of a cable-stayed bridge for dynamic analysis. *Earthquake Engineering and Structural Dynamics*, Vol. **20**, pp. 707 – 721.

[38] **Negrao, J. H. O., Simoes, L. M. C.,** 1997 : Optimization of cable-stayed bridges with three dimensional modelling, *Computers and Structures*, Vol. **64**, No. 1-4, pp. 741-758.

[39] **Simoes, L. M. C., Negrao, J. H. O.,** 2000 : Optimization of cable-stayed bridges with box-girder decks, *Advances in Engineering Software,* Vol. **31**, pp. 417-423.

[40] **Wang, P.H., Lin, H. T., Tang, T. Y.,** 2002 : Study on nonlinear analysis of a highly redundant cable-stayed bridge, *Computers & Structures,* Vol. **8**, No. 2, pp. 165-182.

[41] **Wang, P.H., Tang, T. Y., Zheng, H.N.,** 2004 : Analysis of Cable-Stayed Bridges During Construction by cantilever methods, *Computers & Structures,* Vol. **82**, pp. 329-346.

[42] **Chen, D. W., Au, F. T. K., Tham, L.G., Lee, P.K.K.,** 2000 : Determination of initial cable forces in prestressed concrete cable-stayed bridges for given design deck profiles using the force equilibrium method, *Computers & Structures,* Vol. **74**, pp. 1-9.

[43] **Saadeghvaziri, M. A., Foutch, D. A.,** 1991 : Dynamic Behavior of R/C highway bridges under the combined effect of vertical and horizontal earthquake motions, *Earthquake Engineering and Structural Dynamics,* Vol. **20**, pp. 535 – 549.

[44] **Broderick, B. M., Elnashai, A. S.,** 1995 : Analysis of the failure of the failure of Interstate 10 freeqay ramp during the Northridge earthquake of 17 January 1994, *Earthquake Engineering and Structural Dynamics,* Vol. **24**, No. **2**, pp. 189 – 208.

[45] **Papazoglou, A. J., Elnashai, A. S.,** 1996 : Analytical and field evidence of the damaging effect of vertical earthquake ground motion, *Earthquake Engineering and Structural Dynamics,* Vol. **25**, pp. 1109 – 1137.

[46] **Yu, C. P.,** 1996 : Effect of vertical earthquake componenets on bridge responses, *Ph.D. Thesis,* University of Texas at Austin, Texas.

[47] **Yu, C. P., Broekhuizen, D. S., Roesset, J. M., Breen, J. E., Kreger, M. E.,** 1997 : Effect of vertical ground motion on bridge deck response, *Proceedings, Workshop on Earthquake Engineering Frontiers in Transportation Facilities*, Techical Report No. NCEER-97-0005, National Center for Earthquake Engineering Research, State Universtiy of New York at Buffalo, N. Y., 249 - 263.

[48] **Button, M. R., Cronin, C. J., Mayes, R. L.** 2002 : Effect of vertical motions on seismic response of bridges, *Earthquake Engineering and Structural Dynamics*, Vol. **25**, pp. 1109 – 1137.

[49] **Veletzos, M. J., Restrepo, J. I., Seible, F.,** 2006 : Response of precast segmental bridge superstructures, *Report submitted to Caltrans - SSRP-06/18*, University of California, San Diego, California.

[50] **Kunnath, S. K., et al.** 2008 : Development of guidelines for incorporation of vertical ground motion effects in seismic design of highway bridges, *Report No. CA/UCD-SESM-08-01*, University of California, San Diego, California

[51] **Kim, S. J., Curtis, J. H., Elnashai, A. S.,** 2011 : Analytical Assessment of the Effect of Vertical Earthquake Motion on RC Bridge Piers, *Journal of Structural Engineering*, Vol. **137**, No. **2**, pp. 252 – 260.

[52] **Elnashai, A. S., Di Sarno, L.,** 2008 : Fundamentals of Earthquake Engineering: Theory and Design. *John Wiley & Sons*, 2nd Edition.

[53] **Newmark, N. M., Blume, J. A., Kapur, K. K.,** 1973 : Seismic Design Spectra for Nuclear Power Plants, *Journal of the Power Division*, Vol. **99**, pp. 287 – 303.

[54] **Abrahamson, N. A., Lithesiher, J. J.,** 1989 : Attenuation of vertical peak acceleration, *Bulletin of the Seismological Society of America*, Vol. **79**, No. **3**, pp. 549 – 580.

[55] **Ambraseys, S. J., Simpson, K. A.,** 1996 : Prediction of vertical response spectra in Europe, *Earthquake Engineering & Strucutral Dynamics,* Vol. **25**, No. **4**, pp. 401 – 412.

[56] **Elgamal, A., He, L.,** 2004 : Vertical earthquake ground motion records: An overview, *Journal of Earthquake Engineering*, Vol. **8**, No. **5**, pp. 663 – 697.

[57] **Bozorgnia, S. J., Campbell, K. W.,** 1995 : Analysis of the failure of Interstate 10 freeway ramp during the Northridge earthquake of 17 January 1994., *Earthquake Engineering & Strucutral Dynamics*, Vol. **24**, No. **2**, pp. 189 – 208.

[58] **SeismoSignal,** 2010: User’s Manual, SeismoSoft Ltd., Pavia, Italy.

[59] **Collier, C. J., Elnashai, A. S.,** 2001 : A procedure for combining vertical and horizontal seismic action effects, *Journal of Earthquake Engineering*, Vol. **5**, No. **4**, pp. 521 – 539.

CURRICULUM VITAE

Candidate’s full name: Müge Kuleli

Place and date of birth: Tunceli, 09.07.1986

Permanent Address: Ismet Pasa Dist. Nusrat Mayın St. No:27 Çanakkale, Turkey

Universities and Colleges attended:

2004 - 2009 : Istanbul Technical University, Istanbul, Turkey
Faculty of Civil Engineering
BSc., Department: Civil Engineering

2001 - 2004 : Canakkale Science High School, Istanbul, Canakkale
Science and Mathematics